TERMINAL AREA GUIDANCE ALONG CURVED PATHS – A STOCHASTIC CONTROL APPROACH TO DIGITAL FLIGHT COMPENSATION

by

Joseph Edward Quaranta

Submitted in Partial Fulfillment of the Requirements
for the Degree of
Master of Science in Engineering
in the
Electrical Engineering
Program

Robert A. Foulkes Jr 8-16-76
Adviser Date

Dean of the Graduate School 8-17-76
Dean of the Graduate School Date

YOUNGSTOWN STATE UNIVERSITY

August, 1976

ABSTRACT

TERMINAL AREA GUIDANCE ALONG CURVED PATHS-A STOCHASTIC CONTROL APPROACH TO DIGITAL FLIGHT COMPENSATION

Joseph E. Quaranta
Master of Science in Engineering
Youngstown State University, 1976

In this paper, stochastic control theory is applied to the problem of designing a digital flight compensator for terminal area guidance along a helical flight path as a prelude to landing. The development of aircraft, wind and measurement models is discussed along with a control scheme consisting of feedback gains multiplying estimates of the aircraft and wind states obtained from a Kalman one-step predictor. Preliminary results are presented which indicate that the compensator performs satisfactorily in the presence of both steady winds and gusts. Finally, a derivation of the control and predictor equations is presented in the appendix.

ACKNOWLEDGEMENTS

I would like to express my most sincere thanks to all the faculty members and computer center personnel who have helped in completing this research. I would especially like to thank Dr. Robert H. Foulkes, the initiator of this project, for his guidance and patience in helping me understand the principles underlying the topics presented in this thesis. I would also like to thank him for his suggestions concerning the actual writing of the thesis and for the modeling section of this paper. Finally, I would like to thank Mrs. Anna Mae Serrecchio for the many long hours she spent in typing this thesis.

TABLE OF CONTENTS

LIST OF SYMBOLS

$\bar{a}_c$	Inertial acceleration of mass center
A, A_w	Continuous time system matrices, aircraft and wind.
$\bar{A}_B$	Aerodynamic force vector
Az	Azimuth from MLS
$(A)^{-1}$	Inverse of matrix A
b	Aircraft wing span
B, B_w	Continuous time input matrices, aircraft and wind.
c_n	Constant term w.r.t. u_n
cos (x)	Trigonometric cosine of angle x
C, C_w	Measurement matrices, aircraft and wind.
C_A	Augmented measurement matrix
d_n	Constant term w.r.t. u_n
D	Drag force
D_0, D_1, D_{01}, D_{02}	Coefficient matrices in system model
E {x}	Expected value of x
E^i_j	Row vector with j coordinates, all 0 except the i^{th} which is 1.
$E\ell$	Elevation from MLS
$\bar{f}$	Force
F_A	Atmosphere-fixed reference frame
F_E	Earth reference frame
F_I	Inertial reference frame
$\bar{g}_B$	Acceleration due to gravity in body coordinates
G, G_w	Intermediate matrices used in calculating feedback gains H and H_w
$\bar{G}$	External moment vector
$\bar{G}_B$	Body axes moments, [L M N]

$\bar{h}$	External angular momentum vector
h_b	Barometric altimeter
$\dot{h}_b$	Vertical speed indicator
H, H_w	Feedback gains
I	Aircraft moment of inertia matrix
I_x, I_y, I_z, I_{zx}	Components of body axes moments of inertia
J	Cost functional
L	Lift
[L M N]	Components of external moment $\bar{G}_B$
L_{Bw}	Transformation matrix, transforms wind-axes components to body-axes components. In general, L_{yx} transforms vector in x coordinates to a vector in y coordinates.
L_k	Kalman one-step predictor gain matrix
L_u, L_v, L_w	Turbulence scale factors
m	Mass
$\hat{M}$	Discrete-time aircraft-control cost matrix
$\hat{N}$	Discrete-time aircraft-wind cost matrix
p, q, r	Body axis angular velocities
p_g, q_g, r_g	Angular gust velocities
P_k, P_{wk}	Solutions to matrix riccati for system gains H and H_w.
P_{xy}	Cross-covariance matrix of x and y
P_{yy}	Covariance matrix of y
Q, $\hat{Q}$	Aircraft cost matrices, continuous and discrete.
$\mathcal{R}$	Range from MLS
R, $\hat{R}$	Control cost matrices, continuous and discrete.
R	Helix radius
$\tilde{R}$	Intermediate matrix used in calculating feedback gains H and H_w.

δ	Stabilizer
sec (x)	Trigonometric secant of angle x
sin (x)	Trigonometric sine of angle x
t	Time, in seconds.
t_o, t_f	Initial and final time
$\tan^{-1}(x)$	Inverse tangent of number x
tan (x)	Trigonometric tangent of angle x
T	Magnitude of thrust vector
$\overline{T}_B$	Trust vector, body coordinates
u	Control vector
u_g, v_g, w_g	Translational gust velocities
v	Measurement noise
V	Magnitude of velocity vector
$\overline{V}$	Velocity of mass center w.r.t. F_A ($\overline{V} = \overline{V}^A$)
$\overline{V}^I$	Vector quantity $\overline{V}$ measured w.r.t. F_I
$\overline{V}^E$	Vector quantity $\overline{V}$ measured w.r.t. F_E
$\overline{V}_B^E$	Vector quantity $\overline{V}$ measured w.r.t. F_E expressed in F_v coordinates
w, x_w	Wind state vector
$\tilde{w}$, $\tilde{x}$, $\tilde{y}$	Estimation errors of w, x, y.
$\hat{w}$, $\hat{x}$, $\hat{y}$	One-step predicted estimates of w, x, y.
W	Wind velocity w.r.t. F_E ($\overline{w} = \overline{w}^E$)
W_E	East wind component
$\overline{W}_g$	Gust vector
W_N	North wind component
W_R	Radial wind component
$\overline{W}_s$	Steady wind vector
W_T	Tangential wind component

x, δx	Incremental aircraft state vector
$\bar{x}$	Mean value of x
x'	Transpose of x
$\dot{x}$	Time derivative of x, number of dots indicates number of differentiations.
x_{Ak}	Augmented state vector
$\ddot{x}_B$, $\ddot{y}_B$, $\ddot{z}_B$	Body mounted accelerometers
(x_o, y_o)	Ground coordinate of helix center w.r.t. MLS origin
X	Total aircraft state vector
X_e	Equilibrium value of X
y	Incremental measurement vector
Y	Total measurement vector or sideforce
z_E	Vertical earth position
α	Angle of attack
α_T	Angle between thrust vector and x-axis in x-z plane of body axis.
β	Sideslip angle
γ	Angle of elevation
Γ_1	Discrete-time control matrix
Γ_2	Discrete-time coupling matrix
δ_x	Incremental quantity of x
δ_a	Aileron control
δ_e	Elevator control
δ_{kj}	Kroneker delta, = 0 except when k = j then = 1
δ_r	Rudder control
δ_{sp}	Spoiler control
ζ	Gaussian, white, continuous time noise vector
η_k	Discrete-time system noise

θ	Pitch Euler angle
θ_k	Covariance of measurement noise
ν	Helix angle
ξ_{Ak}	Augmented noise vector
ξ_k	Discrete-time system noise
Ξ_k	Covariance of total system noise vector
π	PI or throttle
$\rho(A)$	Spectral radius of A
σ^2	Variance
σ_u, σ_v, σ_w	Translational rms gust velocities
Σ	Summation of mathematical terms to follow
Σ_k	Error covariance
ϕ, ϕ_w	State transition matrices, aircraft and wind.
ϕ	Bank Euler angle
ϕ_A	Augmented state transition matrix
$\phi_x(\omega)$	Power density spectrum of x where x is u_g, v_g, w_g, p_g, q_g and r_g.
χ	Modeling error term
ψ	Heading Euler angle
ω	Angular velocity
A x B	Vector cross-product
$\frac{\partial J}{\partial u}$	Partial derivative of J w.r.t. u
A^*	Denotes optimal value of A
∞	Infinity
$\int_{x_o}^{x_t} f(x)dx$	Integration of f(x) from $x = x_o$ to $x = x_f$

LIST OF FIGURES

1. INTRODUCTION

During the past few decades airports have become more and more the focus of a tremendous amount of activity. As a result, the number of problems associated with airport traffic has risen dramatically. Among the more pressing areas of concern are high noise levels near airports, fuel conservation, and weather-induced delays, diversions, or closures. In order to alleviate some of these problems, NASA and the FAA have jointly initiated a long range research effort, the Terminal Configured Vehicle (TCV) program. Among the objectives of the TCV program are increased capability for zero-visibility operation, reduced air delays and route time, avoidance of sensitive areas, and reduced noise source intensity. These objectives can be met, at least partially, through the development of precise automatic control along steep, curved approach paths. Such paths would allow more efficient scheduling of arriving aircraft, avoidance of sensitive areas, all-weather automatic landings, and reduced noise intensity for areas near airports with a fuel saving over the use of engine acoustic treatment and low approach angles.

A prerequisite to such precise automatic control is the development of improved ground-based navigation and guidance systems along with improved airborne control systems. The ground based improvements in terminal area navigation and guidance will be provided by the Microwave Landing System (MLS). The MLS will periodically provide accurate range, elevation and azimuth information to the on-board control system.

The purpose of this thesis is to present an application of stochastic control theory to the problem of designing an airborne control system

that uses the MLS data for terminal area guidance of a Boeing 737 along a helical flight path as a prelude to landing. A design method is presented which is composed of three steps. First, a system model is presented consisting of an aircraft model, wind model and measurement model. Next, the digital compensator design is presented. Finally, a digital simulation showing the system response using the above compensator is presented.

The modeling chapter of this thesis consists of a brief summary of the development of the system models. This chapter is divided into three sections. The first contains information concerning a perturbation analysis performed on the general, nonlinear equations of flight about a helical equilibrium. The resulting model consists of six degrees of freedom and three kinematic constraints along with three earth positions, three actuator state variables (thrust, throttle and stabilizer) and six contols (throttle rate, stabilizer rate, elevator, rudder, aileron and spoiler).

The second section summarizes the wind model which is composed of a linear system that processes white noise into a state vector whose components exhibit the Dryden spectra. Included in this vector are three linear gust velocities, three rotaional gust velocities and two horizontal steady wind components.

Concluding the modeling chapter is a discussion of the development of a measurement model. The model is comprised of a set of nonlinear equations linking navigation and guidance data obtained from the MLS and on-board sensors to the total states of the aircraft/wind system. Also taken into account are measurement noise effects.

The next chapter of this thesis deals with the design of a digiral compensator. The linear-quadratic-gaussian theory of stochastic optimal

control provides the basis for this design. The compensator is made up of a Kalman predictor, used to obtain estimates of the aircraft and wind states from the measurements, and a set of control gains, used with the above estimates to obtain appropriate control actuator inputs. This section describes the details of the control gain and predictor design.

The final chapter of the thesis deals with a digital simulation of the compensated system. This chapter begins with a discussion of how the simulation is used as a basis for judging the performance of a design and as a tool for "fine tuning" an unsatisfactory design. Following this, preliminary results using the controls obtained by the methods described in chapter 3 are presented for a specified segment of a descending helix. These results indicate that satisfactory control can be obtained in the presence of both gusts and steady winds. Concluding the section is a discussion of the results and of the design method. Included in the discussion are some suggestions for further study and a summary of some of the computational difficulties involved in the present study.

The appendix is used to present an outline of the derivations of the algorithms used to compute the predictor and control gains. This section is heavily documented to provide the interested reader with other sources containing more details of the theory applied in this thesis as well as more detailed mathematical proofs and derivations of the above gains.

2. THE SYSTEM MODELS

In this chapter[1] the aircraft, wind, and measurement models are developed. In Section 2.1, the nonlinear equations of motion are presented and a perturbation model about a helical equilibrium of those equations developed. The wind model, consisting of a linear system subjected to white noise, yielding wind components exhibiting the Dryden spectra, is presented in Section 2.2. Finally, the MLS data as well as on board sensor readings are expressed in terms of state variables and inputs, and a suitable linear measurement model is developed in Section 2.3.

2.1 The Aircraft Model

The following development is carried out assuming the Earth is an inertial system and is locally flat. The notation here follows closely that in Etkin [2]. Thus, F_I and F_E denote inertial and Earth reference frames, respectively, and $\overline{V}^I$ and $\overline{V}^E$ denote a vector quantity $\overline{V}$ measured with respect to F_I and F_E, respectively. Also, $\overline{V}_V^E$ denotes the vector $\overline{V}$ measured with respect to F_E expressed in F_V coordinates. Thus, under the assumptions above, if $\overline{V}$ is the mass center velocity of an aircraft, $\overline{V}_E^E = \overline{V}_V^E$.

Let $\overline{W}$ denote the wind velocity with respect to the Earth (i.e., $\overline{W} = \overline{W}^E$) and let F_A be an atmosphere-fixed reference frame. Also, let $\overline{V}$ denote mass center velocity with respect to F_A (i.e., $\overline{V} = \overline{V}^A$). Then $\overline{V}^E = \overline{W} + \overline{V}$. It will be convenient to express the wind velocity as the sum of a steady wind $\overline{W}_s$ and gust term $\overline{W}_g$. Then $\overline{V}^E = \overline{V} + \overline{W}_s + \overline{W}_g$.

The force equation, $\overline{f} = m\overline{a}_c$, where $\overline{a}_c$ is the mass center inertial

---

[1]The material in this chapter closely follows Foulkes [1].

acceleration and $\bar{f}$ is the external force, will be expressed in the body axis reference frame. Under the assumptions stated above, $\bar{a}_c = \dot{\bar{V}}^E$, so that

$$\bar{a}_{c_B} = \dot{\bar{V}}_B^E + \bar{\omega}_B^B \times \bar{V}_B^E \,,^1$$

where $\bar{\omega}_B^B = [p\ q\ r]'$[2] is the angular velocity and $\bar{V}_B^E$ is the mass center inertial velocity, both expressed along body axes.

In order to use airspeed V, angle of attack α, and sideslip angle β as state variables, $\bar{V}_B$ is expressed as $L_{BW}\,\bar{V}_W$, where $\bar{V}_W = [V\ 0\ 0]'$ and L_{BW} transforms wind-axes components into body-axis components (see [2]). Then

$$\bar{a}_{c_B} = \frac{d}{dt}\left(L_{BW}\,\bar{V}_W + L_{BV}\,\bar{W}_{s_V} + \bar{W}_{g_B}\right)$$

$$+ \bar{\omega}_B^B \times \left(L_{BW}\,\bar{V}_W + L_{BV}\,\bar{W}_{s_V} + \bar{W}_{g_B}\right)$$

$$= \frac{d}{dt}\left(L_{BW}\,\bar{V}_W\right) + \bar{\omega}_B^B \times L_{BW}\,\bar{V}_W + \dot{\bar{W}}_{g_B} + \bar{\omega}_B^B \times \bar{W}_{g_B} \qquad (2.1.1)$$

The external force is computed as $\bar{f}_B = \bar{A}_B + m\,\bar{g}_B + \bar{T}_B$, where $\bar{A}_B$ is the aerodynamic force, $\bar{T}_B$ is the thrust, and $m\bar{g}_B$ the gravity force. The scalar components of $\bar{g}_B$ are given by

$$\bar{g}_B = [-\,g \sin\theta \quad g\cos\theta\sin\phi \quad g\cos\theta\cos\phi]'.$$

To get the scalar components of $\bar{T}_B$, it is assumed the thrust vector is in the xz-plane of the body-axis frame and makes an angle α_T with respect to x-axis. Then

$$\bar{T}_B = [T\cos\alpha_T \quad 0 \quad -\,T\sin\alpha_T]'$$

---

[1]The dot notation is used for time differentiation. Thus, $\dot{x}$ means dx/dt.

[2]Vector quantities are treated as column vectors; the prime means transpose.

where T is the thrust magnitude. The aerodynamic force is given in terms of the lift L, sideforce Y, and drag D:

$$\bar{A}_B = L_{BW}\,\bar{A}_W = L_{BW}\begin{bmatrix} -D \\ Y \\ -L \end{bmatrix} .$$

To put the force equations in state variable form, the scalar components of $\bar{a}_{c_B} = \frac{1}{m}\bar{F}_B$ are written out and solved for $\dot{V}$, $\dot{\beta}$, and $\dot{\alpha}$, yielding

$$\begin{aligned}
\dot{V} &= \frac{T}{m}\cos(\alpha+\alpha_T)\cos\beta - \frac{D}{m} \\
&+ g(-\cos\alpha\cos\beta\sin\theta + \sin\beta\cos\theta\sin\phi \\
&+ \sin\alpha\cos\beta\cos\theta\cos\phi) \\
&- \dot{u}_g\cos\alpha\cos\beta - \dot{v}_g\sin\beta - \dot{w}_g\sin\alpha\cos\beta \\
&+ u_g(-r\sin\beta + q\sin\alpha\cos\beta) + v_g(r\cos\alpha\cos\beta - p\sin\alpha\cos\beta) \\
&+ w_g(-q\cos\alpha\cos\beta + p\sin\beta) \qquad (2.1.2a)
\end{aligned}$$

$$\begin{aligned}
\dot{\beta} &= \frac{T}{mV}\cos(\alpha+\alpha_T)\sin\beta + \frac{Y}{mV} \\
&+ \frac{g}{V}(\cos\alpha\sin\beta\sin\theta + \cos\beta\cos\theta\sin\phi - \sin\alpha\sin\beta\cos\theta\cos\phi) \\
&- r\cos\alpha + p\sin\alpha + \frac{\dot{u}_g}{V}\cos\alpha\sin\beta - \frac{\dot{v}_g}{V}\cos\beta \\
&+ \frac{\dot{w}_g}{V}\sin\alpha\sin\beta - \frac{u_g}{V}(r\cos\beta + q\sin\alpha\sin\beta) \\
&+ \frac{v_g}{V}(p\sin\alpha\sin\beta - r\cos\alpha\sin\beta) \\
&+ \frac{w_g}{V}(p\cos\beta + q\cos\alpha\sin\beta) \qquad (2.1.2b)
\end{aligned}$$

$$\begin{aligned}
\dot{\alpha} &= -\frac{T}{mV\cos\beta}\sin(\alpha+\alpha_T) - \frac{L}{mV\cos\beta} \\
&+ \frac{g}{V\cos\beta}(\sin\alpha\sin\theta + \cos\alpha\cos\theta\cos\phi) + q \\
&- r\sin\alpha\tan\beta - p\cos\alpha\tan\beta + \frac{\dot{u}_g}{V\cos\beta}\sin\alpha \\
&- \frac{\dot{w}_g}{V\cos\beta}\cos\alpha + \frac{u_g}{V\cos\beta}(q\cos\alpha) \\
&- \frac{v_g}{V\cos\beta}(p\cos\alpha + r\sin\alpha) + \frac{w_g}{V\cos\beta}(q\sin\alpha) \qquad (2.1.2c)
\end{aligned}$$

Following [2], the vector moment equation is $\bar{G} = \dot{\bar{h}}$, where $\bar{G}$ is the external moment and $\bar{h}$ is the angular momentum. Assuming $\dot{I} = 0$ and neglecting any elastic components of $\bar{h}$, $\bar{h}_B = I\,\bar{\omega}_B^B$, where I denotes the body axes moments of inertia. Then $\bar{G}_B = \dot{\bar{h}}_B + \bar{\omega}_B^B \times \bar{h}_B = I\,\dot{\bar{\omega}}_B^B + \bar{\omega}_B^B \times I\,\bar{\omega}_B^B$. The scalar moment equations are given below for the case of a rigid body with a plane of symmetry, where $\bar{G}_B = [L\ M\ N]'$:

$$L = I_x \dot{p} - I_{zx} \dot{r} - I_{zx}\, pq - (I_y - I_z)qr$$

$$M = I_y \dot{q} - I_z(r^2 - p^2) - (I_z - I_x)\, rp$$

$$N = I_z \dot{r} - I_{zx} \dot{p} - I_{zx}\, qr - (I_x - I_y)\, pq.$$

To arrange in state variable form, the equations are solved for $\dot{p}$, $\dot{q}$, and $\dot{r}$:

$$\dot{p} = \frac{I_{zx}(I_z + I_x - I_y)}{I_x I_z - I_{zx}^2}\, pq + \frac{I_z(I_y - I_z) - I_{zx}^2}{I_x I_z - I_{zx}^2}\, qr$$

$$+ \frac{I_z}{I_x I_z - I_{zx}^2}\, L + \frac{I_{zx}}{I_x I_z - I_{zx}^2}\, N \qquad (2.1.3a)$$

$$\dot{q} = \frac{I_{zx}}{I_y}(r^2 - p^2) + \frac{I_z - I_x}{I_y}\, rp + \frac{1}{I_y}\, M \qquad (2.1.3b)$$

$$\dot{r} = \frac{I_{zx}^2 + I_x(I_x - I_y)}{I_x I_z - I_{zx}^2}\, pq + \frac{I_{zx}(I_x + I_y - I_z)}{I_x I_z - I_{zx}^2}\, qr$$

$$+ \frac{I_{zx}}{I_x I_z - I_{zx}^2}\, L + \frac{I_x}{I_x I_z - I_{zx}^2}\, N \qquad (2.1.3c)$$

Since p, q, and r are components of inertial angular momentum (along body axes), the only wind effects in these equations are the effects of the gust angular velocities p_g, q_g, and r_g on the external

moments L, M, and N, These effects will be taken into account in the development of the perturbation model.

In addition to the six-degrees of freedom presented above, the basic nonlinear model contains three kinematic constraints relating body-axes Euler angle rates to the body-axes angular velocities p, q, and r:

$$\dot{\phi} = p + q \sin\phi \tan\theta + r \cos\phi \tan\theta \qquad (2.1.4a)$$

$$\dot{\theta} = q \cos\phi - r \sin\phi \qquad (2.1.4b)$$

$$\dot{\psi} = (q \sin\phi + r \cos\phi) \sec\theta \qquad (2.1.4c)$$

In order to choose Earth position variables, it is assumed that the helix center is known with respect to some fixed reference point such as the MLS origin. Then the Earth position is described in cylindrical coordinates with origin at the helix center at ground level. The position variables are radius R, angle ν, and vertical Earth position z_E; their rates are given by

$$\begin{aligned}\dot{R} = {} & V(A \cos\nu + \mathcal{B} \sin\nu) - W_R + u_g \cos\theta \cos(\psi - \nu) \\ & + v_g (\sin\phi \sin\theta \cos(\psi - \nu) - \cos\phi \sin(\psi - \nu)) \\ & + w_g (\cos\phi \sin\theta \cos(\psi - \nu) + \sin\phi \sin(\psi - \nu)) \end{aligned} \qquad (2.1.5a)$$

$$\begin{aligned}\dot{\nu} = {} & \frac{V}{R}(\mathcal{B} \cos\nu - A \sin\nu) + \frac{W_T}{R} + \frac{u_g}{R} \cos\theta \sin(\psi - \nu) \\ & + \frac{v_g}{R} (\sin\phi \sin\theta \sin(\psi - \nu) + \cos\phi \cos(\psi - \nu)) \\ & + \frac{w_g}{R} (\cos\phi \sin\theta \sin(\psi - \nu) - \sin\phi \cos(\psi - \nu)) \end{aligned} \qquad (2.1.5b)$$

$$\dot{z}_E = - V \sin\gamma - u_g \sin\theta + v_g \sin\phi \cos\theta + w_g \cos\phi \cos\theta \qquad (2.1.5c)$$

where $A = \cos\alpha \cos\beta \cos\theta \cos\psi + \sin\beta(\sin\phi \sin\theta \sin\psi - \cos\phi \sin\psi)$ $+ \sin\alpha \cos\beta (\cos\phi \sin\theta \cos\psi + \sin\phi \sin\psi)$,

$$\begin{aligned}\mathcal{B} = {} & \cos\alpha \cos\beta \cos\theta \sin\psi + \sin\beta (\sin\phi \sin\theta \sin\psi \\ & + \cos\phi \cos\psi) + \sin\alpha \cos\beta (\cos\phi \sin\theta \sin\psi - \sin\phi \cos\psi),\end{aligned}$$

$$\sin\gamma = \cos\alpha\cos\beta\sin\theta - \sin\beta\sin\phi\cos\theta$$

$$- \sin\alpha\cos\beta\cos\phi\cos\theta,$$

and W_R and W_T are the (inward) radial and tangential components of the steady wind, respectively.

The remaining state variables in the aircraft model result from modeling the thrust-throttle and stabilizer actuator systems. The thrust-throttle relation is modeled as a first-order lag with a time constant of 0.5 second. In addition, the commanded input will be throttle rate, so that throttle position also becomes a state variable. Finally, stabilizer rate is commanded so that stabilizer position is considered a state variable. The relations describing the behavior of these variables are given with the development of the perturbation model.

The nonlinear aircraft model consists of the force equations (2.1.2), the moment equations (2.1.3), the kinematic constraints (2.1.4), the inertial velocity equations (2.1.5), and the actuator state variable equations. The model can be represented as a single nonlinear vector equation

$$\dot{X} = f(X, U, W, \dot{W}),$$

where

$$X = [V\ \beta\ \alpha\ p\ q\ r\ \phi\ \theta\ \psi\ R\ \nu\ z_E\ T\ \pi\ \delta]'$$

is the total state vector,

$$U = [\dot{\pi}\ \dot{\delta}\ \delta_e\ \delta_r\ \delta_a\ \delta_{sp}]'$$

is the input vector, and

$$W = [u_g\ v_g\ w_g\ p_g\ q_p\ r_g\ W_R\ W_T]'$$

is the wind vector.

The perturbation model consists of the first-order terms in a Taylor series expansion of the nonlinear equation about a descending helical equilibrium. The equilibrium is determined under a zero wind condition by

solving the nonlinear equation

$$\dot{X}_e = f(X_e, U_e, 0, 0),$$

where the subscript e denotes an equilibrium value. In order to find a unique solution, additional constraints are provided by choosing equilibrium values for airspeed V_e, bank angle ϕ_e, and angle of elevation γ_e, and by constraining the aircraft to fly a "truly banked" turn [2]. This means that the aircraft angular velocity is constant and vertical and that the sideforce is zero.

The constraint equations were solved numerically for a specified airspeed of 120 knots, bank angle of 15°, and angle of elevation of -3° using data for the Boeing 737 used in the TCV program. In addition, from the 737 data, the first partial derivatives of the force equations (2.1.2), moment equations (2.1.3), and kinematic constraint equations (2.1.4) with respect to V, β, α, p, q, r, ϕ θ, and ψ were evaluated numerically at the equilibrium. These derivatives are the coefficients of V, β, α, p, q, r, ϕ, θ, and ψ in the perturbation model.

The coefficients of the wind terms in the perturbation model as well as all coefficients in the inertial velocity equations (2.1.5) were computed by evaluating the appropriate partial derivatives at the equilibrium. The coefficients of the angular gust velocities p_g, q_g, and r_g in the moment equations were computed by evaluating the partials of the aerodynamic terms with respects to p, q, and r, respectively.

The remaining equations in the perturbation model describe the actuator system state variables, viz,, thrust, throttle, and stabilizer. Other actuator variables (elevator, rudder, aileron, and spoiler), in addition to stabilizer rate and throttle rate, are used as commanded inputs. The thrust-throttle relation is given by

$$\dot{\delta T} = -\frac{1}{2}\delta T + \frac{626.66}{2}\delta\pi$$

where δT is the thrust in pounds from the equilibrium value and $\delta\pi$ is the throttle setting in degrees from the equilibrium throttle setting. The last two equations simply state that throttle rate ($\dot{\pi}$) and stabilizer rate ($\dot{\delta}$) are commanded inputs.

Using the state vector

$$x = [\delta V \ \delta\beta \ \delta\alpha \ \delta p \ \delta q \ \delta r \ \delta\phi \ \delta\theta \ \delta\psi \ \delta R \ \delta\nu \ \delta z_E \ \ \delta T \ \ \delta\pi \ \delta\delta]',$$

the input vector

$$u = [\delta\dot{\pi} \ \delta\dot{\delta} \ \ \delta_e \ \ \delta_r \ \ \delta_a \ \ \delta_{sp}]',$$

and the wind vector

$$W = [u_g \ v_g \ w_g \ p_g \ q_g \ r_g \ W_R \ W_T]',$$

the perturbation model in usual state-variable form is

$$\dot{x} = Ax + Bu + D_{01} w + D_{02} \dot{w} . \qquad (2.1.6)$$

Note that all coordinates of the vectors are perturbations.

In order to minimize the variance in the magnitudes of the entries in the coefficient matrices A, B, D_{01}, and D_{02}, normalized variables are used. The translational velocity variables δV, u_g v_g, w_g, W_R, and W_T are normalized by the equilibrium airspeed V_e. Hence x_1 (the first state variable) $= \frac{\delta V}{V_e}$, e.g., while $w_1 = \frac{u_g}{V_e}$. Also, angular positions and velocities are expressed in radians and radians/second. The helix radius is normalized by the equilibrium radius R_e, so that $x_{10} = \frac{\delta R}{R_e}$. Finally, both vertical Earth position δz_E and thrust δT are normalized by a factor of 1000.

2.2 The Wind Model

As seen in section 2.1, the wind vector in the aircraft model consists of three translational gust velocities u_g, v_g, and w_g; three rotational gust velocities p_g, q_g, and r_g; and two steady wind components W_R and W_T. The gust velocities, all of which are components along the body-axes, are modeled as

having the Dryden spectra and are produced for simulation and filter design purposes by a linear system processing white noise. As an example of the linear system design, consider the gust velocity u_g, normalized by the equilibrium airspeed V_e. The power density spectrum of the normalized u_g is [3]

$$\Phi_{u_g}(\omega) = \frac{2L_u\sigma_u^2}{V_e^3} \quad \frac{1}{1 + (\frac{L_u}{V_e}\omega)^2}$$, where σ_u is the rms gust velocity in ft/sec, L_u is a turbulence scale factor in feet, and ω is the frequency variable in rad/sec.

Now, if a linear system with transfer function

$$H(j\omega) = \frac{1}{1 + j\omega \frac{L_u}{V_e}}$$

is subjected to a white noise input with variance $\sigma^2 = \frac{2L_u\sigma_u^2}{V_e^3}$, the output is a random process with the spectrum $\Phi_{u_g}(\omega)$ [4]. A system with the required transfer function is described in state-variable form by

$$\dot{x}_{w1} = \frac{-V_e}{L_u} x_{w1} + \frac{V_e}{L_u} \zeta_1 ,$$

$$w_1 = x_{w1} ,$$

where ζ_1 is a mean zero white noise process with variance $\frac{2L_u\sigma_u^2}{V_e^3}$, x_{w1} is a state variable, and w_1 is the output having the required spectrum.

The remaining gust velocities are generated in a similar manner. The spectra of the gust components are shown in Table 2.2.1.

As indicated in the previous section, W_R and W_T are the radial and tangential components of the steady wind (figure 2.2.1), which are related to the north wind W_N and east wind W_E by the spiral angle ν:

	VELOCITY	SPECTRUM*
Translational	u_g	$\frac{2L_u\sigma_u^2}{V_e^3} \frac{1}{1+(\frac{L_u}{V_e}\omega)^2}$
	v_g	$\frac{L_v\sigma_v^2}{V_e^3} \frac{1+3(\frac{L_v}{V_e}\omega)^2}{1+(\frac{L_v}{V_e}\omega)^2{}^2}$
	w_g	$\frac{L_w\sigma_w^2}{V_e^3} \frac{1+3(\frac{L_w}{V_e}\omega)^2}{1+(\frac{L_w}{V_e}\omega)^2{}^2}$
Rotational	p_g	$\frac{0.8\sigma_w^2}{L_w V_e} \frac{(\frac{\pi L_w}{4b})^{\frac{1}{3}}}{1+(\frac{4b}{\pi V_e}\omega)^2}$
	q_g	$\frac{\omega^2}{1+(\frac{4b}{\pi V_e}\omega)^2} \Phi_{w_g}(\omega)$
	r_g	$\frac{\omega^2}{1+(\frac{3b}{\pi V_e})^2} \Phi_{v_g}(\omega)$

Table 2.2.1. Gust Spectra (Dryden)

*L_u, L_v, L_w are turbulence scale factors. b is the aircraft wing span. V_e is equilibrium airspeed. σ_u, σ_v, σ_w are rms translational gust velocities.

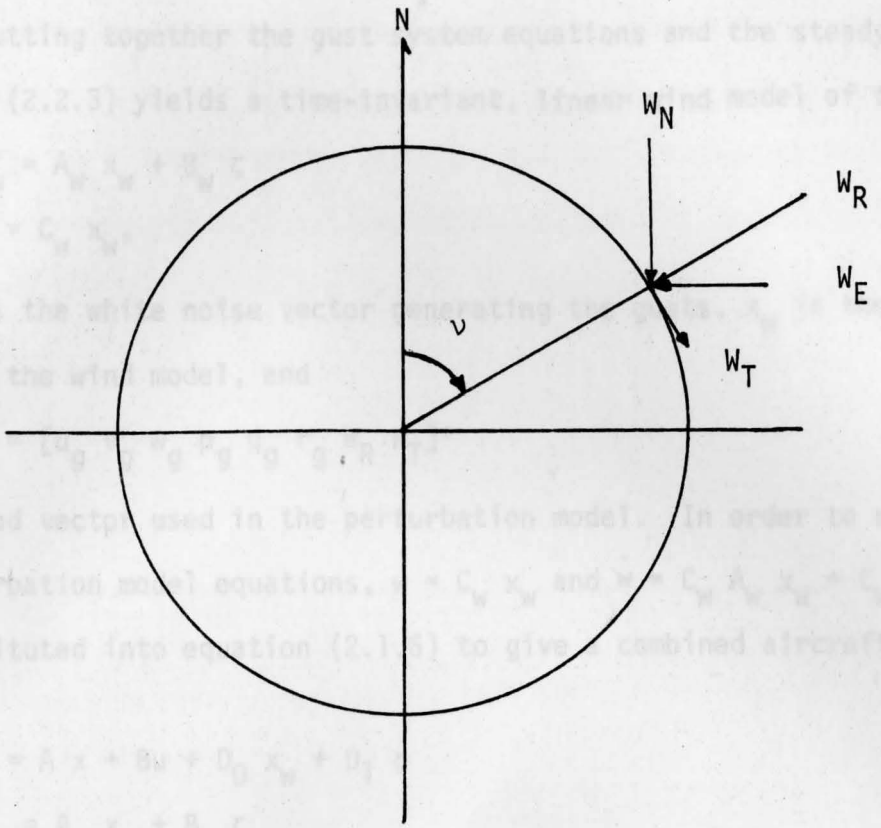

Figure 2.2.1. Steady Wind Components

$$W_R = W_N \cos \nu + W_E \sin \nu \tag{2.2.1}$$

$$W_T = W_N \sin \nu - W_E \cos \nu$$

Thus, $\dot{W}_R = - \dot{\nu} W_T$ and $\dot{W}_T = \dot{\nu} W_R$. (2.2.2)

For simulation purposes, north and east winds are selected and W_R and W_T are computed using equations (2.2.1). For the filter design, because a constant coefficient wind model is desired and the equilibrium wind is zero, equations (2.2.2) are approximated by

$$\dot{W}_R = - \dot{\nu}_e W_T$$

$$\dot{W}_T = \dot{\nu}_e W_R \ , \tag{2.2.3}$$

where $\dot{\nu}_e$ is the equilibrium spiral angle rate, which is constant and equal to $V_e \cos \gamma_e / R_e$.

Putting together the gust system equations and the steady wind equations (2.2.3) yields a time-invariant, linear wind model of the form

$$\dot{x}_w = A_w x_w + B_w \zeta$$
$$w = C_w x_w,$$

where ζ is the white noise vector generating the gusts, x_w is the state vector of the wind model, and

$$w = [u_g \; v_g \; w_g \; p_g \; q_g \; r_g \; W_R \; W_T]'$$

is the wind vector used in the perturbation model. In order to use x_w in the perturbation model equations, $w = C_w x_w$ and $\dot{w} = C_w A_w x_w + C_w B_w \zeta$ are substituted into equation (2.1.6) to give a combined aircraft/wind model:

$$\dot{x} = A x + Bu + D_0 x_w + D_1 \zeta$$
$$\dot{x}_w = A_w x_w + B_w \zeta \qquad (2.2.4)$$

where $D_0 = D_{01} C_w + D_{02} C_w A_w$ and $D_1 = D_{02} C_w B_w$.

2.3 The Measurement Model

Measurements available for control purposes consist of the MLS data (range, azimuth, and elevation) and a number of on-board sensor readings. The total measurement vector is

$$Y = [\mathcal{R} \; Az \; E\ell \; p \; q \; r \; \phi \; \theta \; \psi \; V \; h_b \; \dot{h}_b \; \ddot{x}_B \; \ddot{y}_B \; \ddot{z}_B]'$$

where $\mathcal{R}$, Az, $E\ell$ are the MLS data; p, q, r are angular velocities from rate gyros; ϕ, θ, ψ are bank angle, pitch, and heading from position gyros; V is an airspeed indicator reading, h_b and $\dot{h}_b$ are barometric altimeter and vertical speed indicator readings; and $\ddot{x}_B$, $\ddot{y}_B$, $\ddot{z}_B$ are body-mounted accelerometer readings.

The total measurements are computed for simulation purposes by computing the total state variables as equilibrium values plus increments

and expressing the measurements in terms of the states. In order to compute the MLS data, it is assumed that r, Az, and El are measured with respect to a common origin and that the helix center is known with respect to that origin. If the ground coordinates of the helix center with respect the MLS origin are (x_o, y_o), then (see figure 2.3.1)

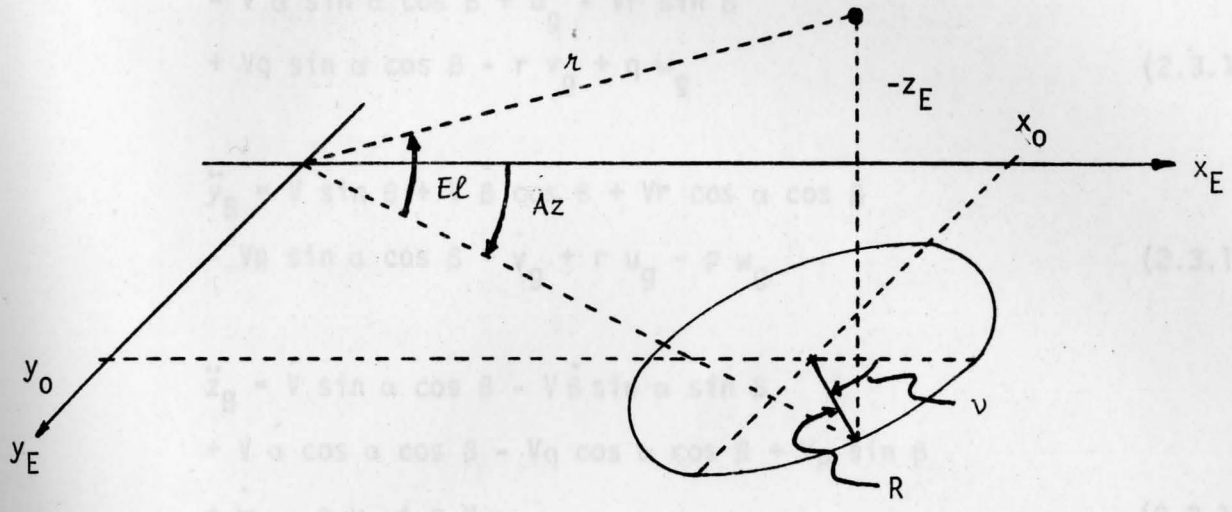

Figure 2.3.1. MLS Coordinates Definitions

$$r = \sqrt{(x_o + R\cos\nu)^2 + (y_o + R\sin\nu)^2 + z_E^2}\ ,$$

$$Az = \tan^{-1}\left[\frac{y_o + R\sin\nu}{x_o + R\cos\nu}\right],$$

$$El = \tan^{-1}\left[\frac{-z_E}{\sqrt{(x_o + R\cos\nu)^2 + (y_o + R\sin\nu)^2}}\right],$$

where R, ν, and z_E are coordinates 10, 11, and 12 of the total state vector (see p. 9).

The fourth through tenth measurements are the same as total states. Also $h_b = -z_E$ and $\dot{h}_b = -\dot{z}_E = V_e \sin \gamma_e - 1000.\ \dot{x}_{12}$, where the derivative $\dot{x}_{12}$ is computed from equation (2.2.4). Finally, expressions for the accelerometer readings are obtained by writing out the scalar components of the acceleration $\bar{a}_{c_B}$ from equation (2.1.1):

$$\ddot{x}_B = \dot{V} \cos\alpha \cos\beta - V\dot{\beta} \cos\alpha \sin\beta - V\dot{\alpha} \sin\alpha \cos\beta + \dot{u}_g - Vr \sin\beta + Vq \sin\alpha \cos\beta - r v_g + q w_g \qquad (2.3.1a)$$

$$\ddot{y}_B = \dot{V} \sin\beta + V\dot{\beta} \cos\beta + Vr \cos\alpha \cos\beta - Vp \sin\alpha \cos\beta + \dot{v}_g + r u_g - p w_g \qquad (2.3.1b)$$

$$\ddot{z}_B = \dot{V} \sin\alpha \cos\beta - V\dot{\beta} \sin\alpha \sin\beta + V\dot{\alpha} \cos\alpha \cos\beta - Vq \cos\alpha \cos\beta + Vp \sin\beta + \dot{w}_g - q u_g + p v_g . \qquad (2.3.1c)$$

In the simulation, the measurements are generated using the above formulas along with random noise effects. Except for the airspeed and vertical speed indicators, the noise is an additive, white, mean zero Gaussian process with standard deviation as shown in Table 2.3.1 (see [5] and [6]). The airspeed and vertical speed indicator noises are multiplicative, where the indicated measurement is obtained by multiplying the actual measurement by a normal random variable of mean 1 and standard deviation as given in Table 2.3.1.

The incremental measurements to be used with the perturbation model are to be of the form

$$y = C\ x + C_w\ x_w + v,$$

where v is a noise term and x and x_w are the aircraft and wind model state

MEASUREMENT	NOISE STANDARD DEVIATION
Range	1 foot
Azimuth	0.41×10^{-3} rad
Elevation	0.61×10^{-3} rad
Rate gyros (p, q, r)	0.1 deg/sec[1]
Bank gyro	0.5 deg/sec[1]
Pitch gyro	0.15 deg/sec[1]
Heading gyro	1. deg/sec[2]
Airspeed	$.02^2$
Barometric altimeter	27.5 feet[2]
Vertical speed indicator	$.05^2$
Accelerometer ($\ddot{x}_B$, $\ddot{z}_B$)	(.005) 32.2 ft/sec^2 [1]
Accelerometer ($\ddot{y}_B$)	(.0005) 32.2 ft/sec[1]

Table 2.3.1. Measurement Noise Standard Deviations

[1]See reference [5]

[2]See reference [6]

vectors, respectively. These measurements are processed from the total measurement vector y discussed above. The first 12 coordinates of the incremental measurement vector y are given below.

$$y_1 = \frac{\delta R}{R_e} = x_{10}$$

$$y_2 = \delta\nu = x_{11}$$

$$y_3 = \frac{\delta z_E}{1000.} = x_{12}$$

$$y_K = x_K, \quad K = 4,5,\ldots, 9$$

$$y_{10} = \frac{\delta V}{V_e} = x_1$$

$$y_{11} = \frac{\delta h_b}{1000.} = - x_{12}$$

$$y_{12} = \frac{\dot{\delta h}_b}{V_e} = - \dot{x}_{12} \frac{1000.}{V_e} = - \frac{1000.}{V_e} E_{12}^{15} (Ax + D_0 x_w) \quad ,$$

where E_i^j denotes a row vector with j coordinates, all 0 except the i^{th}, which is 1. The last three incremental measurements are derived from the accelerometer readings by expanding the acceleration equations (2.3.1) about equilibrium values, keeping through first-order terms only, and defining the measurement as the difference between the total acceleration and the terms in the expansion involving the equilibrium values and controls. Thus,

$$\begin{aligned}
\ddot{x}_B = &- V_e r_e \sin\beta_e + V_e q_e \sin\alpha_e \cos\beta_e \\
&+ \cos\alpha_e \cos\beta_e \, \dot{\delta V} - V_e \cos\alpha_e \sin\beta_e \, \dot{\delta\beta} \\
&- V_e \sin\alpha_e \cos\beta_e \, \dot{\delta\alpha} + \dot{u}_g + (-r_e \sin\beta_e + q_e \sin\alpha_e \cos\beta_e) \, \delta V \\
&- V_e (r_e \cos\beta_e + q_e \sin\alpha_e \sin\beta_e) \, \delta\beta \\
&+ V_e q_e \cos\alpha_e \cos\beta_e \, \delta\alpha - V_e \sin\beta_e \, \delta r \\
&+ V_e \sin\alpha_e \cos\beta_e \, \delta q - r_e v_g + q_e w_g .
\end{aligned}$$

Substituting from the perturbation model equations (2.2.4) for the derivatives and putting the control and equilibrium terms on the left-hand side gives

$$y_{13} = \ddot{x}_B + V_e r_e \sin\beta_e - V_e q_e \sin\alpha_e \cos\beta_e$$
$$- V_e \cos\alpha_e \cos\beta_e E_1^{15} Bu + V_e \cos\alpha_e \sin\beta_e E_2^{15} Bu$$
$$+ V_e \sin\beta_e \cos E_e E_3^{15} Bu \qquad (2.3.2a)$$
$$= V_e \cos\alpha_e \cos\beta_e E_1^{15} (Ax + D_o x_w)$$
$$- V_e \cos\alpha_e \sin\beta_e E_1^{15} (Ax + D_o x_w)$$
$$- V_e \sin\alpha_e \cos\beta_e E_1^{15} (Ax + D_o x_w)$$
$$+ V_e (-r_e \sin\beta_e + q_e \sin\alpha_e \cos\beta_e) x_1$$
$$- V_e (r_e \cos\beta_e + q_e \sin\alpha_e \sin\beta_e) x_2$$
$$+ V_e (q_e \cos\alpha_e \cos\beta_e) x_3 + V_e \sin\alpha_e \cos\beta_e x_5$$
$$- V_e \sin\beta_e x_6 + E_1^8 C_w A_w x_w - r_e E_2^8 C_w x_w + q_e E_3^8 C_w x_w \qquad (2.3.2b)$$

The incremental measurements derived from $\ddot{y}_B$ and $\ddot{z}_B$ are handled in a similar way. Finally, the y_{13}, y_{14}, and y_{15} measurements are all normalized by dividing by V_e.

As seen from the above discussion the fifteen incremental measurements are linear functions of x and x_w. Thus, y may be written as

$$y = C x + C_w x_w + v \quad ,$$

where v is a noise term that depends on the noise in the total measurements. This expression for y is used in the filter design later. In the simulation, y is processed from Y by using equations such as (2.3.2a) for the accelerations and by subtracting equilibrium values from total measurements in the other cases. For y_1, y_2, and y_3, total helix radius R, helix

angle ν, and vertical Earth position z_E must be calculated from range, azimuth, and elevation. The equations are

$$R = \sqrt{(r \cos E\ell \cos Az - x_o)^2 + (r \cos E\ell \sin Az - y_o)^2}$$

$$\nu = \tan^{-1}\left[\frac{r \cos E\ell \sin Az - y_o}{r \cos E\ell \cos Az - x_o}\right]$$

$$z_E = - r \sin E\ell \ .$$

The noise effects in the incremental measurements are assumed to be white, mean zero Gaussian processes with standard deviations that are the same as for the total measurements except for the noise terms in y_1, y_2, y_3, y_{10}, and y_{12}. Since $y_{10} = (1 + E_v)\ V$, where V is total airspeed and E_v is a mean zero Gaussian random variable with 0.02 standard deviation, the standard deviation of the perturbation airspeed was approximated by 0.02 V_e. Similarly, the standard deviation of the perturbation sink rate was approximated by 0.05 times the equilibrium sink rate.

The standard deviations in the helix radius, helix angle, and altitude perturbations derived from the MLS data were approximated using the standard deviations of the MLS data. For a helix radius of about 5000 feet, an initial altitude of 3000 feet, and helix center ground coordinates of $x_o = 0$ and $y_o = 2R_e$, the altitude standard deviation was approximated by the maximum range times the standard deviation in the elevation. This result was rounded to 10 feet. The radius standard deviation was approximated by the average distance to the helix ground track times the standard deviation in the azimuth. This result was rounded to 5 feet. Finally, the helix angle standard deviation was approximated by the standard deviation in the azimuth, multiplied by the ratio of the maximum distance to the helix ground track to the nominal helix radius, and the result rounded to 10^{-3} radian.

3. THE DESIGN OF A CONTROL SYSTEM

Using the aircraft, wind and measurement models presented in the previous section the problem can be restated mathematically as a variation of the Linear-Quadratic-Gaussian (LQG) problem of stochastic control. It can be classified as a time-invariant, linear, stochastic regulator problem.

The total system, including the aircraft, wind and measurement models, can be mathematically stated as follows:[1]

$$\dot{x}(t) = A\,x(t) + Bu(t) + D_0 w(t) + D_1 \zeta(t) \tag{3.1}$$

$$\dot{w}(t) = A_w w(t) + B_w \zeta(t) \tag{3.2}$$

$$y(t) = C\,x(t) + C_w w(t) + v(t) \tag{3.3}$$

for $t_o < t < t_f$

where x, u, w and y are the state, control, wind disturbance and measurement vectors respectively, v(t) is a white, gaussian vector of measurement noise and $\zeta(t)$ is a white, gaussian noise vector that drives the wind system and corrupts the aircraft system. The other matrices (A, B, D_0, D_1, A_w, B_w, C and C_w) are time-invariant with appropriate dimensions.

The next step is to establish some criteria against which we can judge the performance of the solution. For the regulator problem we use a quadratic cost functional of the form

$$J = \frac{1}{2} E\left\{\int_{t_o}^{t_f} [x'(t)\,Qx(t) + u'(t)\,Ru(t)]\,dt\right\} \tag{3.4}$$

where E is the expectation operator, the prime denotes the transpose, and both Q and R are positive definite, time-invariant weighting matrices.

---

[1] All quantities are small-signal.

The problem can now be stated as follows. Given the linear system of equations (3.1-3.3), find a control u such that the cost functional J of equation (3.4) is minimized.

The first step in solving this problem is to transform the system of equations (3.1-3.4) into their discrete-time equivalents. This is done for several reasons. First, a digital compensator is desired since the on-board computer is digital and any control algorithm must be compatible with a digital system. Secondly, the MLS data is only provided periodically. Therefore, the measurement system is inherently a discrete-time one. Finally, a digital simulation is used to test each design. Therefore, the discrete-time equivalent difference equations make the simulation very easy to implement on a digital computer.

The equivalents are obtained by integrating the system differential equations and cost functional over each sampling period [7]. This can be seen by examining the linear differential equations (3.1) and (3.2). For bounded $u(t)$, $t_o < t < t_f$, the well-known solution is of the form:

$$x(t) = \phi(t,t_o)\, x(t_o) + \int_{t_o}^{t} \phi(t,s)Bu(s)ds$$

$$+ \int_{t_o}^{t} \phi(t,s)D_o\, \phi_w(s,t_o)w(t_o)ds$$

$$+ \int_{t_o}^{t} \left[\phi(t,s)D_1 + \left(\int_{s}^{t} \phi(t,\alpha)D_o\, \phi_w(\alpha,s)d\alpha \right) B_w \right] \zeta(s)ds \qquad (3.5)$$

$$w(t) = \phi_w(t,t_o)w(t_o) + \int_{t_o}^{t} \phi_w(t,s)B_w \zeta(s)ds \qquad (3.6)$$

where $\phi_w(t,t_o)$ and $\phi(t,t_o)$ are state transition matrices which satisfy differential equations of the form:

$$\frac{d}{dt}\ \phi(t,s) = A(t)\ \phi(t,s) \qquad t > s$$

$$\phi(s,s) = I \qquad \text{where I is the identity matrix.}$$

The discrete-time equivalents of (3.1) and (3.2) can now be obtained from (3.5) and (3.6) by changing the interval of integration from $[t_o,t]$ to $[t_k,t_{k+1}]$. If we restrict u(t) to be constant over the sampling period (i.e. $u(t) = u(t_k)$ for $t_k < t < t_{k+1}$), the resultant discrete-time equations are [7]

$$x_{k+1} = \phi x_k + \Gamma_2 w_k + \Gamma_1 u_k + \xi_k \qquad (3.7)$$

$$w_{k+1} = \phi_w w_k + \eta_k \qquad (3.8)$$

where $x_k = x(t_k)$, $u_k = u(t_k)$, $w_k = w(t_k)$, and

$$\phi = \phi(t_{k+1}, t_k) = e^{A(t_{k+1}-t_k)} \qquad (3.9a)$$

$$\phi_w = \phi_w(t_{k+1}, t_k) = e^{A_w(t_{k+1}-t_k)} \qquad (3.9b)$$

$$\Gamma_1 = \Gamma_1(t_{k+1}, t_k) = \left[\int_{t_k}^{t_{k+1}} \phi(t_{k+1},s)ds\right] B \qquad (3.9c)$$

$$\Gamma_2 = \Gamma_2(t_{k+1}, t_k) = \int_{t_k}^{t_{k+1}} \phi(t_{k+1},s)D_o\ \phi_w(s,t_k)ds \qquad (3.9d)$$

$$\xi_k = \xi(t_{k+1},t_k) = \int_{t_k}^{t_{k+1}} \left[\phi(t_{k+1},s)D_1 + \left(\int_s^{t_{k+1}} \phi(t_{k+1},\alpha)D_o\, \phi_w(\alpha,s)d\alpha \right) B_w \right] \zeta(s)ds \qquad (3.9e)$$

$$\eta_k = \eta(t_{k+1},t_k) = \int_{t_k}^{t_{k+1}} \phi_w(t_{k+1},s)B_w\, \zeta(s)ds \qquad (3.9f)$$

Note that in the general time-varying case these equations must be computed for each time interval. However, since the problem considered here possesses time-invariant system matrices and a fixed sampling period, the corresponding discrete-time equivalent matrices are time-invariant.

The discrete-time equivalent measurement equation can be obtained directly from the continuous time equation:

$$y_k = Cx_k + C_w w_k + v_k \qquad (3.10)$$

where $v_k = v(t_k)$ and $y_k = y(t_k)$.

Finally, the discrete-time equivalent of the cost functional (3.4) can be written as a sum of n integrals similar to those in equation (3.9). Using (3.5), the resultant expression for the cost functional becomes [7,8]

$$J = \frac{1}{2} E \{ \sum_{k=o}^{n} x'_{k+1} \hat{Q}\, x_{k+1} + 2x'_{k+1} \hat{N}\, w_{k+1} + 2x'_k \hat{M} u_k + u'_k \hat{R} u_k \} \qquad (3.11)$$

where the new cost matrices are given by:

$$\hat{Q} = \hat{Q}_k = \int_{t_k}^{t_{k+1}} \phi'(t,t_k)Q\, \phi(t,t_k)dt \qquad (3.12a)$$

$$\hat{M} = \hat{M}_k = \int_{t_k}^{t_{k+1}} \phi'(t,t_k) Q \Gamma_1(t,t_k) dt \qquad (3.12b)$$

$$\hat{R} = \hat{R}_k = \int_{t_k}^{t_{k+1}} \left[R + \Gamma_1'(t,t_k) Q \Gamma_1(t,t_k) \right] dt \qquad (3.12c)$$

$$\hat{N} = \hat{N}_k = \int_{t_k}^{t_{k+1}} \phi'(t,t_k) Q \Gamma_2(t,t_k) dt \qquad (3.12d)$$

Once again, note that since the original system and cost matrices are time-invariant the discrete-time cost matrices are time-invariant.

An interesting feature of this cost functional is the presence of cross terms in the form of $\hat{M}$ and $\hat{N}$. These come about because the physical system to be controlled is continuous and the original cost functional penalizes the state variables and controls continuously not just at the sampling instants.

Another, more subtle example of this phenomena can be found by examining $\hat{Q}$ and $\hat{R}$. In this case, as in most cases, the weighting matrices Q and R are chosen to be diagonal. This is done mainly because off-diagonal terms have very little physical meaning. However, even for diagonal Q and R, the discrete-time equivalents $\hat{Q}$ and $\hat{R}$ will contain off-diagonal terms. These terms, like the above cross terms, arise from the fact that the original model of the physical system is continuous.

The problem can now be restated as follows. Find a control sequence $\{u_k\}$ which minimizes the cost functional J in equation (3.11) subject to the constraints that the state equations (3.7,3.8,3.10) must be satisfied; and that u_k must explicitly depend only on the past

measurements $y_0, y_1, y_2, \ldots, y_{k-1}$ when $\{v_k\}$ is a zero-mean, gaussian, white noise sequence independent of $\{[\xi_k', \eta_k']'\}$. In addition it must be stipulated that u be constant over the sampling period.

The above system of equations (3.7,3.8,3.10,3.11)can be augmented to obtain a form very similar to the discrete LQG problem. However, if the normal method of solution is applied, an important difficulty surfaces. The total system may be unstable and uncontrollable due to an unstable wind system. Therefore, if the augmented system is solved with an unstable wind system, the solution to the Riccati equation diverges due to the presence of unstable and uncontrollable poles. But, under certain conditions the gains will be bounded.

It can be shown (see [8] and Appendix A) that the solution to the stochastic optimal control problem described previously exists and is given by:

$$u_k^* = - H_k \hat{x}_k - H_{wk} \hat{w}_k \tag{3.13a}$$

$$H_k = \tilde{R}_k^{-1} G_k, \; H_{wk} = \tilde{R}_k^{-1} G_{wk}, \; \tilde{R}_k = \hat{R} + \Gamma_1' P_k \Gamma_1 \tag{3.13b}$$

$$G_k = \Gamma_1' P_k \phi + \hat{M}' \quad , \quad G_{wk} = \Gamma_1' (P_{wk} \phi_w + P_k \Gamma_2) \tag{3.13c}$$

$$P_{k-1} = \phi' P_k \phi + \hat{Q} - G_k' \tilde{R}_k^{-1} G_k, \; P_n = \hat{Q} \tag{3.13d}$$

$$P_{wk-1} = (\phi - \Gamma_1 \tilde{R}_k^{-1} G_k)' (P_{wk} \phi_w + P_k \Gamma_2) + \hat{N}, \; P_{wn} = \hat{N} \tag{3.13e}$$

where $\hat{x}_k$ and $\hat{w}_k$ are one-step predicted estimates of x_k and w_k given by:

$$\hat{x}_k = E\{x_k | y_{k-1}\} \text{ and } \hat{w}_k = E\{w_k | y_{k-1}\} \tag{3.14}$$

It should be noted that the above gain equations remain valid for any i-step predicted estimate (where i = 0 represents a filtered estimate).

The one-step prediction was used here in order to account for computational delays present in the on-board computer.

Also, the equations above are of a recursive nature. Therefore, at each sampling instant a new optimal gain is calculated. To implement this would require storing all the intermediate values of each gain matrix. This, in turn, would require a greater amount of storage than is normally available for small, on-board computers. For these reasons, a suboptimal design was used consisting of only the steady state gains obtained when the index on the recursive relations tends to infinity.

For the linear, time-invariant problem considered here these steady-state gains are bounded if P_k and P_{wk} converge or if all the poles of the aircraft system are less than one, and if the product

$$\rho(\phi_w)\rho(\phi - \Gamma_1 H) < 1 \qquad (3.15)$$

where $\rho(S)$ denotes the spectral radius of S, and H represents the steady state value of H_k. In other words, the existance of a solution depends on the amount of instability present in the wind system and the degree to which the aircraft system has been stabilized. The more stable the closed loop system is the greater the instability tolerable in the wind system. This can be seen by noting that ϕ_w may have unstable poles up to $1/\rho(\phi - \Gamma_1 H)$. Therefore, as $n \to \infty$ the gains H_k and H_{wk} approach their steady state values H and H_w since P_k and P_{wk} both converge to their steady state values P and P_w.

Finally, it should be emphasized that the optimal control for a system with disturbances consists of two parts. The first part feeds back state estimates multiplied by an optimal gain H_k. This gain is exactly the same as would have been calculated with no disturbance present. The second term feeds back the disturbance estimates multiplied

by a gain H_{wk}, which depends on the disturbance.

The next step is to obtain the state and wind estimate. This is accomplished by first augmenting the discrete-time equations (3.7,3.8,3.10) Then, a one-step Kalman predictor is used on the augmented system to obtain $\hat{x}_{k+1}$ and $\hat{w}_{k+1}$. The results of augmenting (3.7,3.8,3.10) are:

$$\begin{bmatrix} x_{k+1} \\ \hline w_{k+1} \end{bmatrix} = \begin{bmatrix} \phi & \Gamma_2 \\ \hline 0 & \phi_w \end{bmatrix} \begin{bmatrix} x_k \\ \hline w_k \end{bmatrix} + \begin{bmatrix} \Gamma_1 \\ \hline 0 \end{bmatrix} u_k + \begin{bmatrix} \xi_k \\ \hline \eta_k \end{bmatrix} + \chi \qquad (3.16)$$

$$y_k = [C \mid C_w] \begin{bmatrix} x_k \\ \hline w_k \end{bmatrix} + v_k \qquad (3.17)$$

where χ is a white noise term representing modeling error, the significance of which is discussed later.

Given the past measurements y_k, it can be shown (see Appendix B) that the one-step predicted estimates of x_{k+1} and w_{k+1} are given by the equations below:

$$\begin{bmatrix} \hat{x}_{k+1} \\ \hline \hat{w}_{k+1} \end{bmatrix} = \begin{bmatrix} \phi & \Gamma_2 \\ \hline 0 & \phi_w \end{bmatrix} \begin{bmatrix} \hat{x}_k \\ \hline \hat{w}_k \end{bmatrix} + \begin{bmatrix} \Gamma_1 \\ \hline 0 \end{bmatrix} u_k + L_k \left[y_k - [C \mid C_w] \begin{bmatrix} \hat{x}_k \\ \hline \hat{w}_k \end{bmatrix} \right] \qquad (3.18)$$

where $\hat{x}_o = m_o \triangleq E\{x_o\}$, $\hat{w}_o = 0$, and

$$L_k = \begin{bmatrix} \phi & \Gamma_2 \\ \hline 0 & \phi_w \end{bmatrix} \Sigma_k [C \mid C_w]' \left[[C \mid C_w] \Sigma_k [C \mid C_w]' + \theta_k \right]^{-1} \qquad (3.19)$$

where $\Sigma_k = E\left\{ \begin{bmatrix} \tilde{x}_k \\ \hline \tilde{w}_k \end{bmatrix} \begin{bmatrix} \tilde{x}_k \\ \hline \tilde{w}_k \end{bmatrix}' \right\}$, $\begin{bmatrix} \tilde{x}_k \\ \hline \tilde{w}_k \end{bmatrix} = \begin{bmatrix} x_k \\ \hline w_k \end{bmatrix} - \begin{bmatrix} \hat{x}_k \\ \hline \hat{w}_k \end{bmatrix}$ is the estimation

error and Σ_k can be found by solving the Riccati type equation:

$$\Sigma_{k+1} = \left[\begin{array}{c|c} \phi & \Gamma \\ \hline \bar{0} & \bar{\phi}_w \end{array}\right] \left[\Sigma_k - \Sigma_k [C|C_w]' \left[[C|C_w] \Sigma_k [C|C_w]' + \theta_k \right]^{-1} [C\ C_w]\Sigma_k \right]$$

$$\left[\begin{array}{c|c} \phi & \Gamma \\ \hline \bar{0} & \bar{\phi}_w \end{array}\right]' + \Xi_k \qquad (3.20)$$

with $\Sigma_o \triangleq E\left\{ \begin{bmatrix} x_o \\ \bar{w}_o \end{bmatrix} \begin{bmatrix} x_o \\ \bar{w}_o \end{bmatrix}' \right\}$

where $\Xi_k\, \delta_{kj} = E\left\{ \begin{bmatrix} \xi_k \\ \bar{\eta}_k \end{bmatrix} \begin{bmatrix} \xi_k \\ \bar{\eta}_k \end{bmatrix}' \right\}$, $\theta_k\, \delta_{kj} = E\{v_k\ v_j'\}$ (3.21a)

and, $E\left\{ v_k \begin{bmatrix} \xi_j \\ \bar{\eta}_j \end{bmatrix}' \right\} = E\left\{ v_k \begin{bmatrix} x_o \\ \bar{w}_o \end{bmatrix}' \right\} = E\left\{ \begin{bmatrix} \xi_k \\ \bar{\eta}_k \end{bmatrix} \begin{bmatrix} x_o \\ \bar{w}_o \end{bmatrix}' \right\} = 0$ (3.21b)

for all k, j = 0, 1, 2, ...

It must be noted that, as with the control equations, these equations are recursive. For the same reasons discussed previously, a suboptimal predictor was implemented using only the steady state solutions to the above equations.

The total system can now be represented by the block diagram figure 3.1. A more detailed diagram is shown in figure 3.2.

Now that the optimal controls have been defined for specific cost matrices the main concern becomes testing to see if the chosen cost matrices lead to an acceptable system response or if they must be modified to achieve this goal. The digital simulation described in the next section will provide the final step of the design procedure satisfying the above testing and modification requirements.

However, before the simulation is discussed, an important relationship between the Kalman estimator and the closed-loop aircraft system will now be presented. It is well known that in a sampled-data

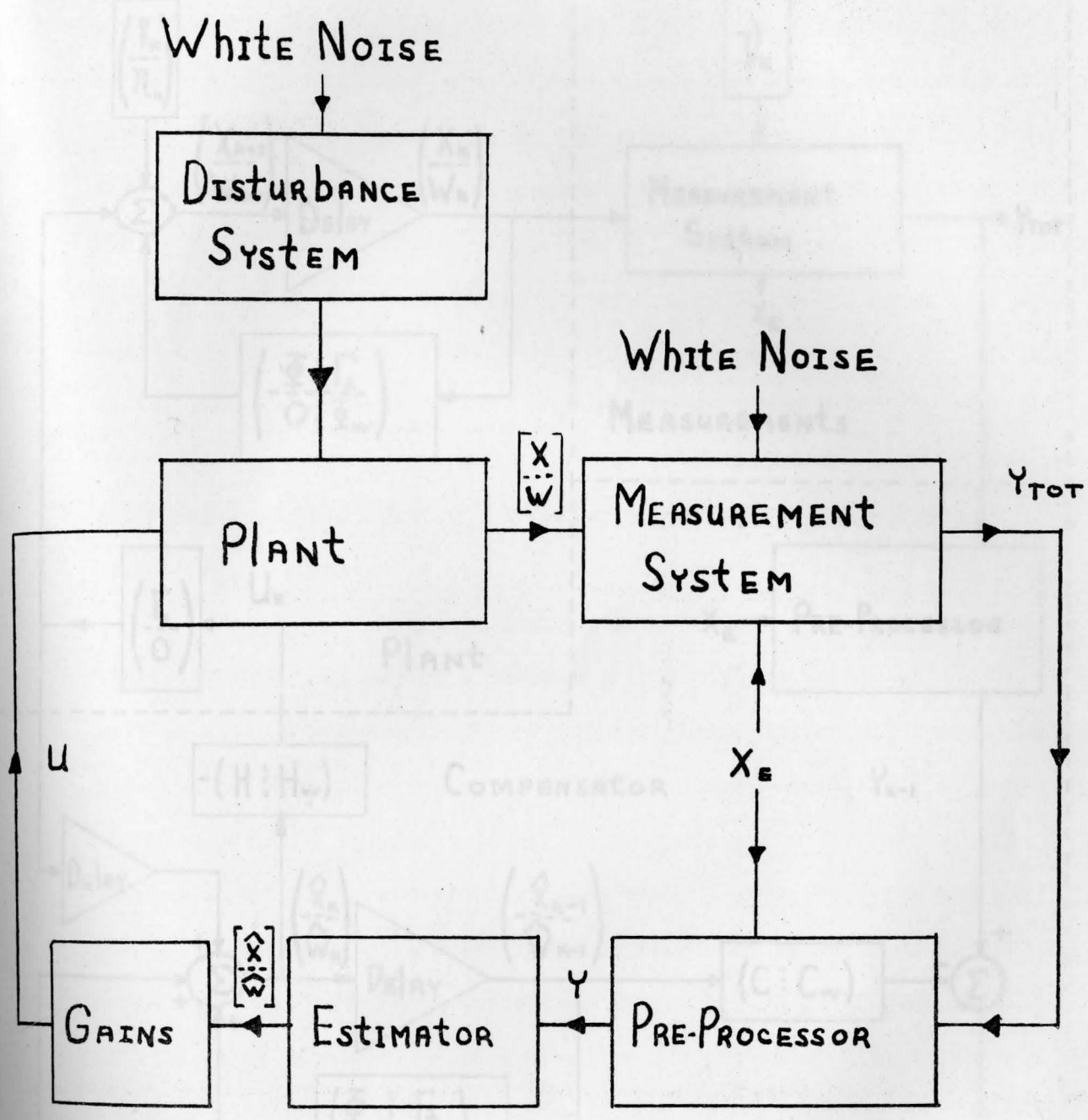

Figure 3.1. Block Diagram of the System.

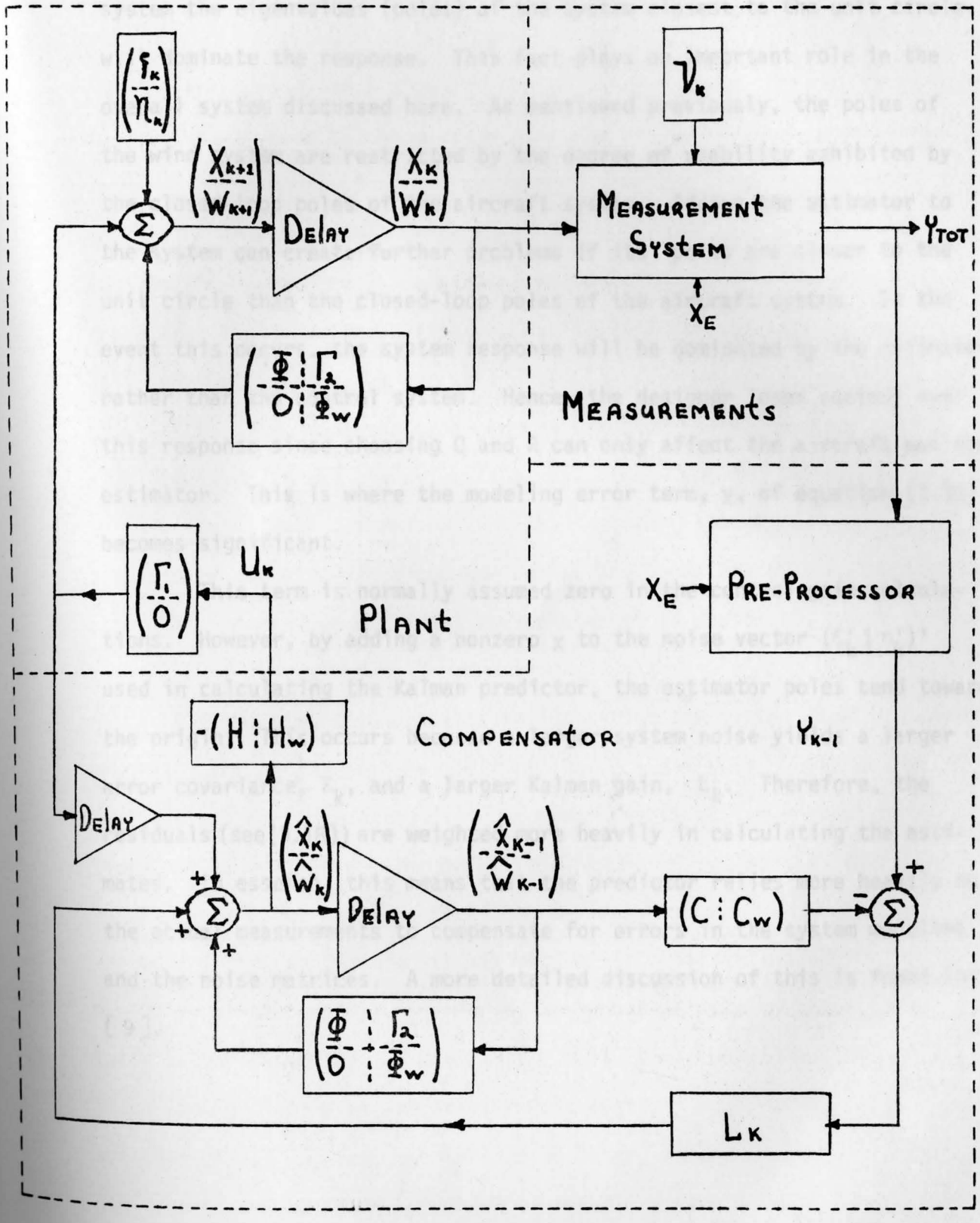

Figure 3.2. Detailed Block Diagram of the System.

system the eigenvalues (poles) of the system closest to the unit circle will dominate the response. This fact plays an important role in the overall system discussed here. As mentioned previously, the poles of the wind system are restricted by the degree of stability exhibited by the closed-loop poles of the aircraft system. Adding the estimator to the system can create further problems if its poles are closer to the unit circle than the closed-loop poles of the aircraft system. In the event this occurs, the system response will be dominated by the estimator rather than the control system. Hence, the designer loses control over this response since choosing Q and R can only affect the aircraft not the estimator. This is where the modeling error term, χ, of equation (3.16) becomes significant.

This term is normally assumed zero in the control gain calculations. However, by adding a nonzero χ to the noise vector $(\xi_k' \vdots \eta_k')'$ used in calculating the Kalman predictor, the estimator poles tend toward the origin. This occurs because a larger system noise yields a larger error covariance, Σ_k, and a larger Kalman gain, L_k. Therefore, the residuals (see(3.18)) are weighted more heavily in calculating the estimates. In essence, this means that the predictor relies more heavily on the actual measurements to compensate for errors in the system modeling and the noise matrices. A more detailed discussion of this is found in [9].

4. SIMULATION

The purpose of a digital simulation is twofold. First, it is used as a method of testing the design. The simulation provides information concerning the response of the aircraft to various winds and initial deviations from the equilibrium positions in addition to how well the equilibrium condition is maintained in the presence of winds once the transients have subsided. Since actual aircraft tests would be impractical, this information provides the only criterion for judging a particular set of weights. The responses obtained are compared to the original design specifications to see how well, if at all, these specifications are met. In this case it was determined that the important specifications are the position of the aircraft along the helix, the bank, the pitch, the airspeed and the absence of large, sudden changes in any of the state variables.

If the simulation results indicate that the system doesn't respond properly, the design must be modified (New Q's and R's). However, an analytic method of choosing Q and R doesn't exist at the present time. Therefore, Q and R are selected by trial-and-error using the simulation results as a guide to "fine-tune" the design.

In this application it was determined, by trial-and-error, that the rates of movement (p, q, r) play an important role in obtaining a satisfactory response. By keeping the roll, yaw, and pitch rates close to their equilibrium values the aircraft system's other state variables are more damped and less susceptable to large, sudden deviations. This can be seen in the various simulation results presented next.

The results are organized to show the various performances obtainable with this design method and the tradeoffs associated with

each design. The first results presented[1] (Figs. 4.1, 4.2, 4.3), show the adaptability of the control system to increasing steady winds. The simulations were run with 10, 20 and 40 feet per second (fps) northerly winds respectively, all other parameters remaining constant. Note how as the steady wind increases, a cyclic mode becomes apparent in the bank angle, heading and spiral angle. This is due mainly to the fact that as the aircraft traverses the helix, the magnitudes of the radial and tangential components of the steady winds are constantly changing. Therefore, in order to maintain a circular ground track, the other variables must compensate. Note, how well the radius, and altitude are kept very close to their optimum values. Also note, in each case the response obtained is fairly smooth and damped.

The next simulation results presented (Fig. 4.4) show how well the aircraft captures the helical mode from a straight and level mode. Although this may be exceeding the linearity region of the system model, the results provide valuable information concerning the settling time of the design. Note that all the transients have disappeared after a period of 10-20 seconds or approximately 1/8 revoltuion around the helix. Another important specification is overshoot. In figure 4.4 overshoot is minimal with the exception of the bank angle (Fig. 4.4a). The overshoot present in the bank angle is a little large although acceptable. Since the bank angle affects passenger comfort, this design may need modification in this area. However, the positional variables (radius and altitude) were emphasised in this design and their response exhibits small

---

[1]In all the results, both the estimates and the actual values of each state variable are plotted on each graph; time is in seconds, angular quantaties are in degrees, and linear quantitites are in feet.

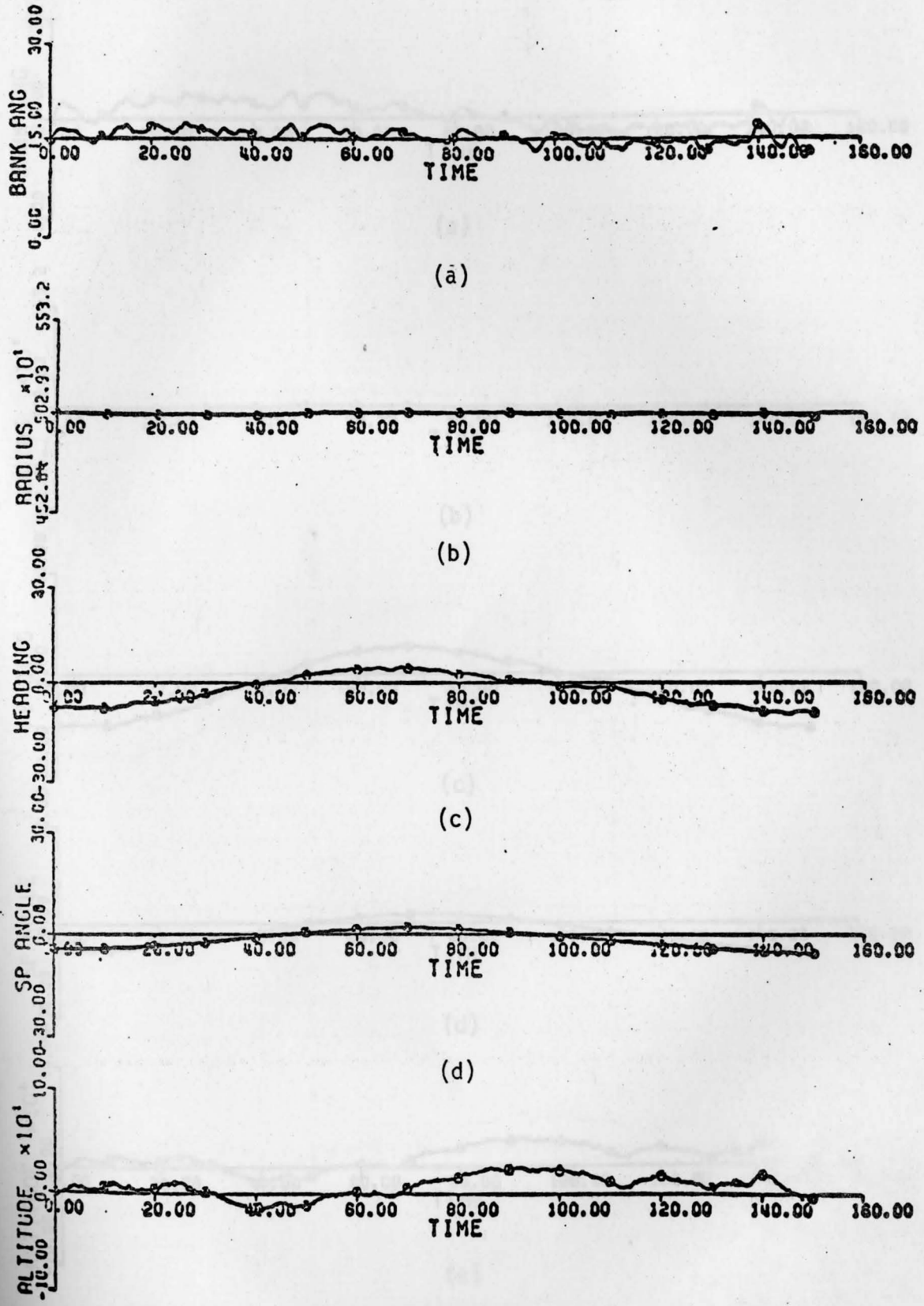

Figure 4.1. Aircraft Simulation (10 fps Steady Winds)

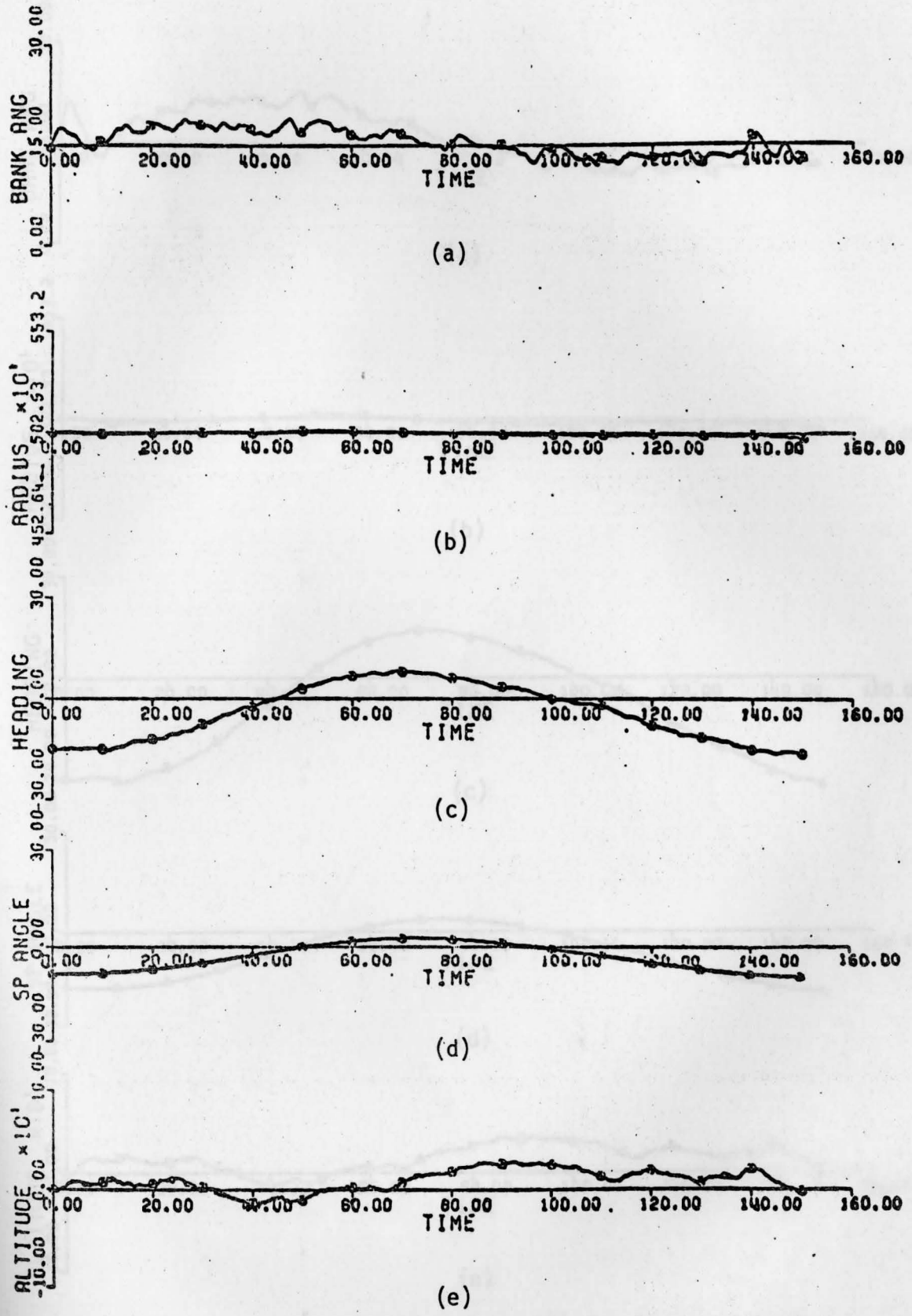

Figure 4.2. Aircraft Simulation (20 fps Steady Winds)

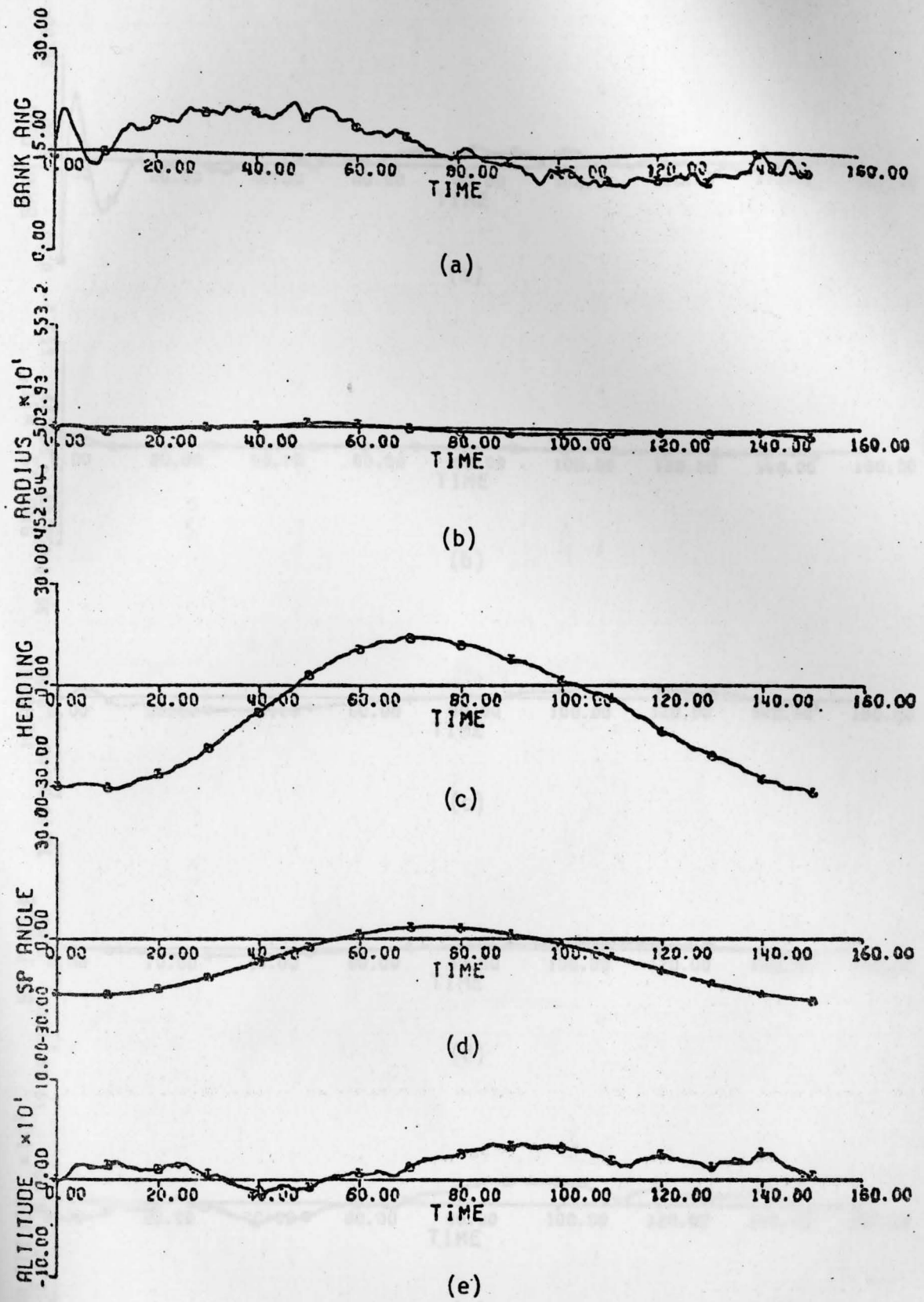

Figure 4.3. Aircraft Simulation (40 fps Steady Winds)

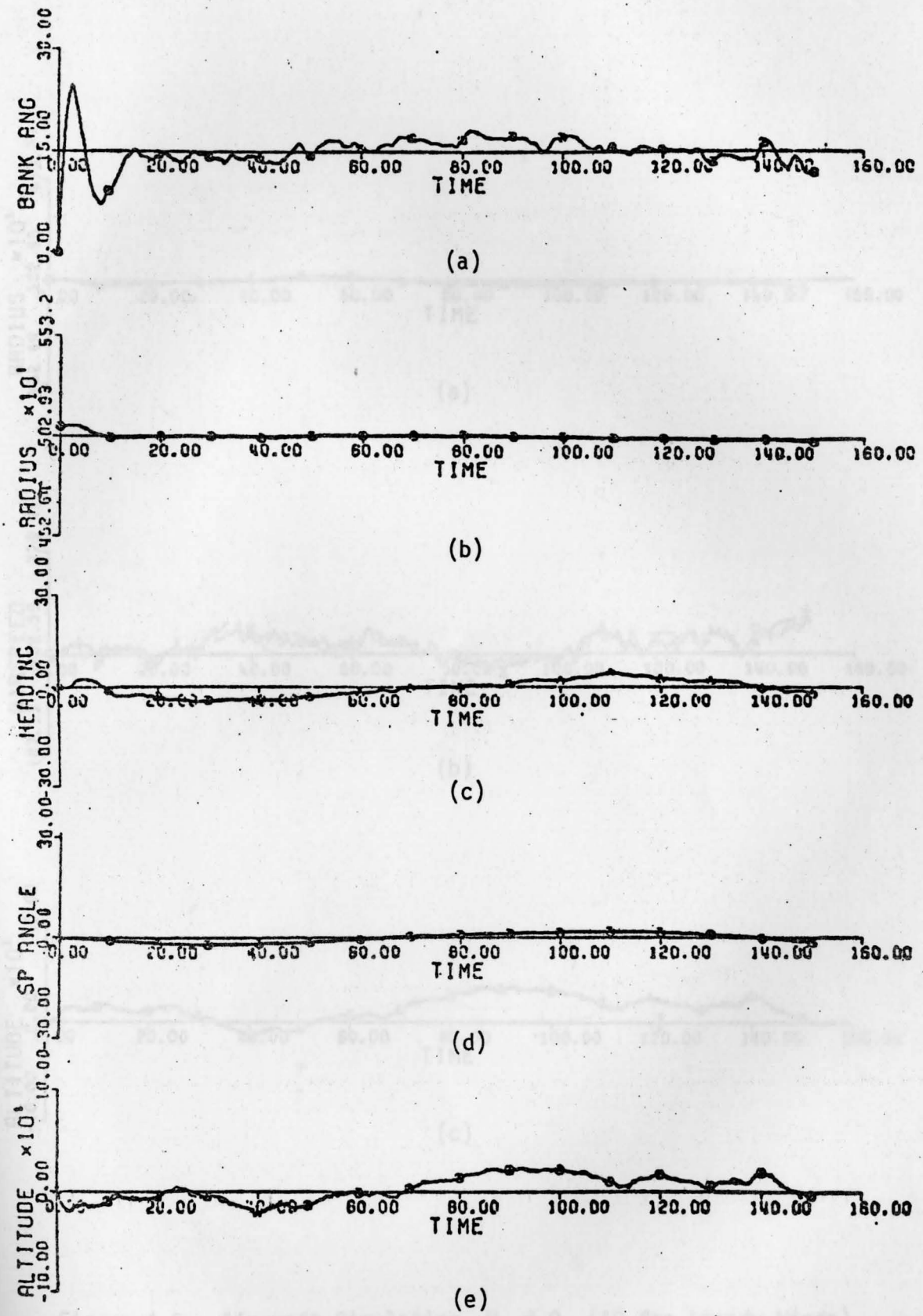

Figure 4.4. Aircraft Simulation, Capture, (10 fps Steady Winds)

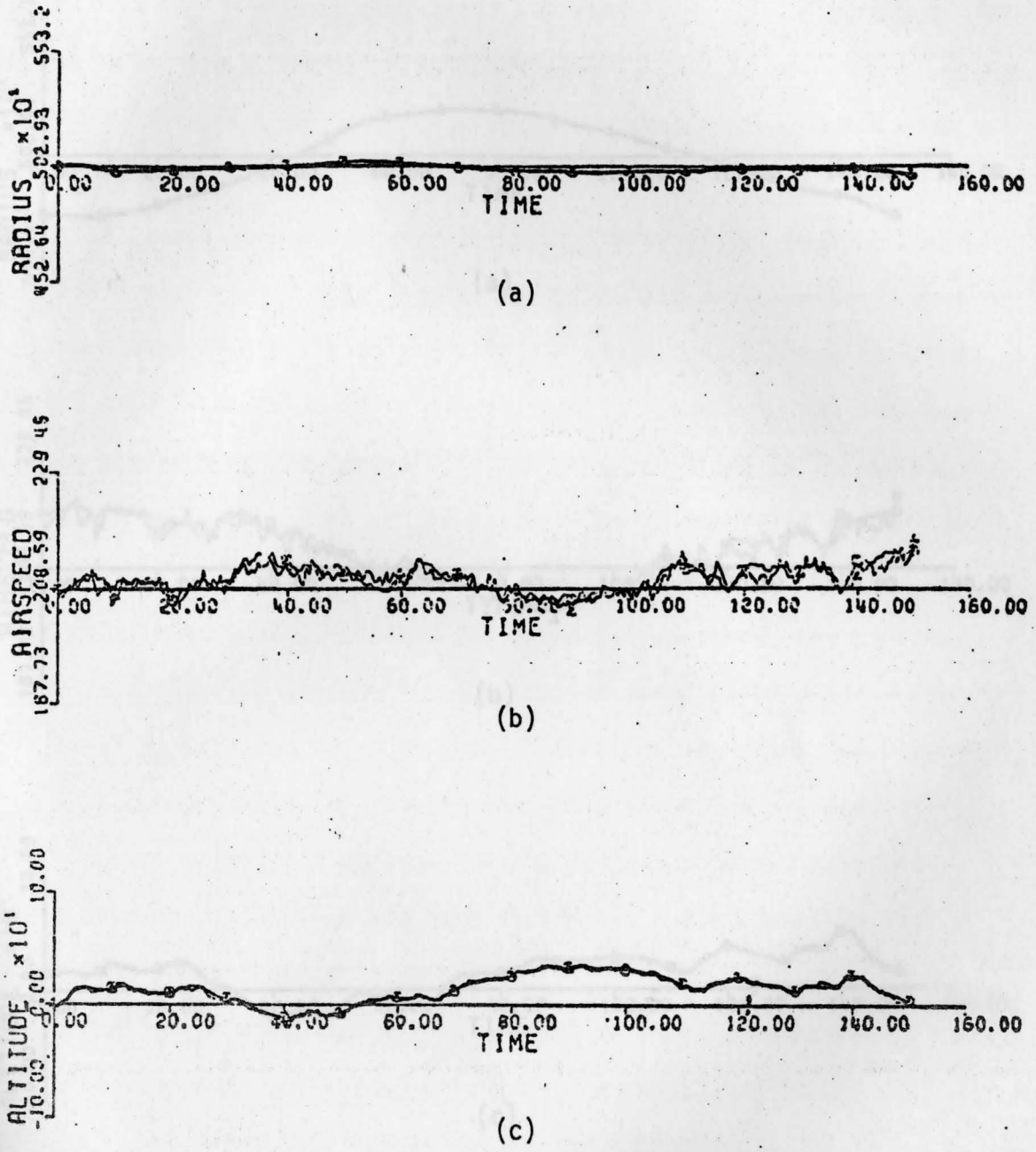

Figure 4.5. Aircraft Simulation, $H_w \neq 0$, (40 fps Steady Winds)

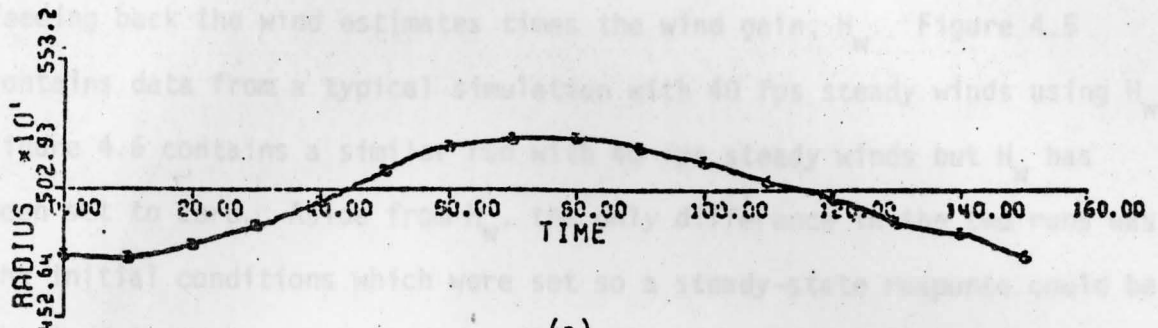

(a)

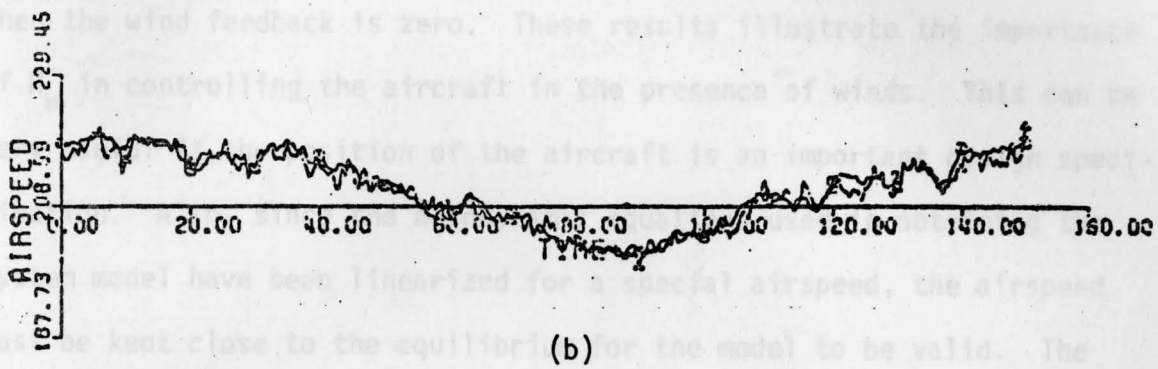

(b)

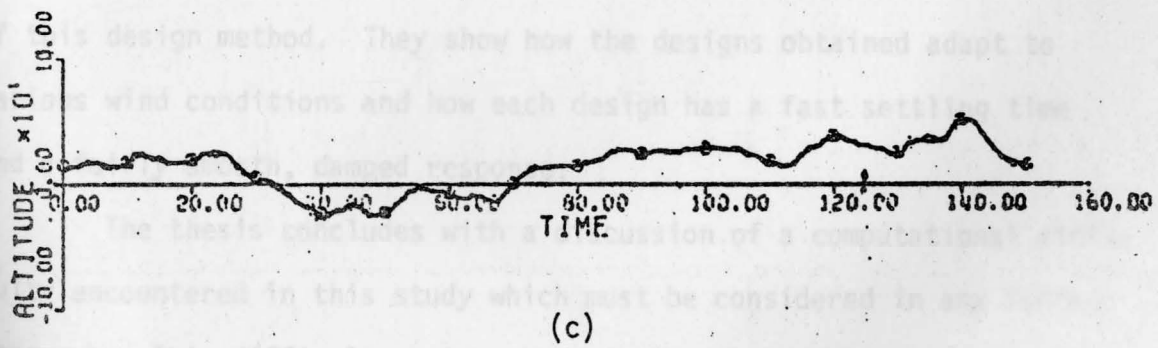

(c)

Figure 4.6. Aircraft Simulation, H_w = 0, (40 fps Steady Winds)

overshoot, fast settling time and small steady-state error.

The final set of results presented illustrated the importance of feeding back the wind estimates times the wind gain, H_w. Figure 4.5 contains data from a typical simulation with 40 fps steady winds using H_w. Figure 4.6 contains a similar run with 40 fps steady winds but H_w has been set to zero. Aside from H_w, the only difference in the two runs was the initial conditions which were set so a steady-state response could be obtained in each case. Note how the airspeed, and radius exhibit greater deviations when $H_w = 0$. Even the altitude deviation is slightly larger when the wind feedback is zero. These results illustrate the importance of H_w in controlling the aircraft in the presence of winds. This can be very useful if the position of the aircraft is an important design specification. Also, since the aerodynamic equations used in obtaining the system model have been linearized for a special airspeed, the airspeed must be kept close to the equilibrium for the model to be valid. The addition of H_w improves this response as shown in the figures 4.5 and 4.6.

In summary, all the results presented here show the versatility of this design method. They show how the designs obtained adapt to various wind conditions and how each design has a fast settling time and a fairly smooth, damped response.

The thesis concludes with a discussion of a computational difficulty encountered in this study which must be considered in any further research. This difficulty arises out of the numerous computations involved in solving a matrix Riccati equation for a large system. Because of this great number of calculations, the accuracy of the solution is suspect. Therefore, it is very important to use the most accurate mode of variable for the computer solution. For example, an IBM 370/145 was

used in this study and it was necessary to resort to double precision variables in order to obtain sufficient accuracy (2 to 2 1/2 digits) in calculating the Kalman one-step predictor. This must be kept in mind when extending this study to cover other helical paths (steeper), other bank angles or any different equilibrium conditions in general.

Another extension of this research which could prove valuable is the modification of the control system gains to improve the system response in the presence of larger gusts. This ability was not exhibited by the designs shown in this thesis but would only require further trial-and-error experimentation with the system weighting matrices.

APPENDIX A

An outline of a method for deriving the optimal control algorithm is presented in this section. For more detailed derivations and precise mathematical proofs, references [8] through [16] can be consulted. The approach taken here follows [8].

Consider the last term in the summation (3.11) for k = n:

$$J_n(u_n) = \frac{1}{2} E \left\{ x'_{n+1} P_n x_{n+1} + 2x'_{n+1} P_{wn} w_{n+1} + 2x'_n \hat{M} u_n + u'_n \hat{R} u_n \right\} \quad \text{(A-1)}$$

where the boundary conditions $P_n = \hat{Q}$ and $P_{wn} = \hat{N}$ have been used. But, x_{k+1} and w_{k+1} are given by (3.7) and (3.8). Substitution yields:

$$\begin{aligned} J_n = \frac{1}{2} E \{ & (\phi x_n + \Gamma_2 w_n + \Gamma_1 u_n + \xi_n)' P_n (\phi x_n + \Gamma_2 w_n + \Gamma_1 u_n + \xi_n) \\ & + 2(\phi x_n + \Gamma_2 w_n + \Gamma_1 u_n + \xi_n)' P_{wn} (\phi_w w_n + n_n) \\ & + 2x'_n \hat{M} u_n + u'_n \hat{R} u_n \} \end{aligned} \quad \text{(A-2)}$$

The above can be simplified by use of the fact that the state noise and the state and control are uncorrelated or:

$$E\{x_n \xi'_n\} = E\{x_n n'_n\} = E\{u_n \xi'_n\} = E\{u_n n'_n\} = 0 \quad \text{(A-3)}$$

since they all have zero mean values.

Using this and noting that Q is symmetric, (A-2) can be expanded to yield:

$$\begin{aligned} J_n = \frac{1}{2} E \{ & x'_n (\phi' P_n \phi) x_n + 2x'_n \phi' (P_n \Gamma_2 + P_{wn} \phi_w) w_n + \\ & 2u'_n (\Gamma'_1 P_n \phi + \hat{M}') x_n + 2u'_n \Gamma'_1 (P_n \Gamma_2 + P_{wn} \phi_w) w_n \\ & + u'_n (\hat{R} + \Gamma'_1 P_n \Gamma_1) u_n \} + c_n \end{aligned} \quad \text{(A-4)}$$

where all the terms not dependent on u_n have been lumped in c_n as follows:

$$c_n = \frac{1}{2} E \{ w_n' \Gamma_2' [P_n \Gamma_2 + 2P_{wn} \phi_w] w_n + \xi_n' P_n \xi_n$$

$$+ 2 \xi_n' (P_n \Gamma_2 + P_{wn} \phi_w) w_n + 2 w_n' \Gamma_2' P_{wn} \eta_n + 2 \xi_n' P_{wn} \eta_n \} \qquad \text{(A-5)}$$

Since c_n depends only on w_n, ξ_n and η_n, and these are independent of u_n, c_n will be dropped from consideration in the minimization procedure. Also, x_n depends only on u_{n-1}. Therefore, the minimization of (A-4) yields:

$$\frac{\partial J_n}{\partial u_n} = \frac{1}{2} E \{ 2(\Gamma_1' P_n \phi + \hat{M}') x_n + 2 \Gamma_1' (P_n \Gamma_2 + P_{wn} \phi_w) w_n$$

$$+ 2(\hat{R} + \Gamma_1' P_n \Gamma_1) u_n \} = 0 \qquad \text{(A-6)}$$

Since u_n is a deterministic function, we have:

$$E \{ u_n \} = u_n \qquad \text{(A-7)}$$

and (A-6) becomes:

$$u_n^* = - (\hat{R} + \Gamma_1' P_n \Gamma_1)^{-1} \left[(\Gamma_1' P_n \phi + \hat{M}') E \{ x_n \} \right.$$

$$\left. + \Gamma_1' (P_n \Gamma_2 + P_{wn} \phi_w) E \{ w_n \} \right] \qquad \text{(A-8)}$$

where * denotes optimality.

This equation can be further simplified using the definitions of G_n, G_{wn} and $\tilde{R}_n$ in (3.13) and a property of the conditional expected value:

$$E \{ x_n \} = E \{ E \{ x_n | y_{n-1} \} \} = E \{ \hat{x}_n \} = \hat{x}_n \qquad \text{(A-9a)}$$

$$E \{ w_n \} = E \{ E \{ w_n | y_{n-1} \} \} = E \{ \hat{w}_n \} = \hat{w}_n \qquad \text{(A-9b)}$$

to obtain:

$$u_n^* = - \tilde{R}_n^{-1} [G_n \hat{x}_n + G_{wn} \hat{w}_n] \qquad \text{(A-10)}$$

Note that u_n^* depends only on y_{n-1}. Therefore, (A-9) is justified. Also, the inverse will exist provided $\hat{R}$ is positive definite and $\hat{Q} = P_n$ is positive semi-definite.

If we substitute this expression for u_n^* back into (A-4) we obtain:

$$J_n^* = \frac{1}{2} E \{x_n' \phi' P_n \phi x_n + 2x_n' \phi' (P_n \Gamma_2 + P_{wn} \phi_w) w_n - 2\hat{x}_n' (G_n' \tilde{R}_n^{-1} G_n) x_n$$

$$- 2\hat{w}_n' (G_{wn}' \tilde{R}_n^{-1} G_n) x_n - 2\hat{x}_n' (G_n' \tilde{R}_n^{-1} G_{wn}) w_n - 2\hat{w}_n' (G_{wn}' \tilde{R}_n^{-1} G_{wn}) w_n$$

$$+ \hat{x}_n' (G_n' \tilde{R}_n^{-1} G_n) \hat{x}_n + \hat{x}_n' (G_n' \tilde{R}_n^{-1} G_{wn}) \hat{w}_n + \hat{w}_n' (G_{wn}' \tilde{R}_n^{-1} G_n) \hat{x}_n$$

$$+ \hat{w}_n' (G_{wn}' \tilde{R}_n^{-1} G_{wn}) \hat{w}_n \} + c_n \qquad \text{(A-11)}$$

where the definitions of (3.13) have been used to simplify the expression.

Next, we define estimation error as follows:

$$\tilde{x}_n = x_n - \hat{x}_n \ , \quad \tilde{w}_n = w_n - \hat{w}_n \qquad \text{(A-12)}$$

using these definitions and noting that the error and the estimate of the state are uncorrelated, zero-mean variables (i.e. $E\{\hat{x}_n' \tilde{x}_n\} = E\{\tilde{x}_n' L \hat{w}_n\} = E\{\tilde{w}_n' \hat{w}_n\} = 0$), it can be shown that:

$$E\{x_n' L w_n\} = E\{\tilde{x}_n' L \tilde{w}_n\} + E\{\hat{x}_n' L \hat{w}_n\} \qquad \text{(A-13)}$$

Also, note that $E\{\tilde{x}_n \tilde{x}_n'\}$, $E\{\tilde{x}_n \tilde{w}_n'\}$ and $E\{\tilde{w}_n \tilde{w}_n'\}$ do not depend on the control sequence $\{u_i\}$ for gaussian processes [16]. Therefore, adding these terms to (A-11) will not affect the optimization results. Doing this and making use of (A-13), we can rewrite (A-11) to yield:

$$J_n^* = \frac{1}{2} E \{x_n' [\phi' P_n \phi - G_n' \tilde{R}_n^{-1} G_n] x_n + 2x_n' \phi' [P_n \Gamma_2 + P_{wn} \phi_w] w_n$$

$$- w_n' (G_{wn}' \tilde{R}_n^{-1} G_n) x_n - x_n' (G_n' \tilde{R}_n^{-1} G_{wn}) w_n \} + d_n \qquad \text{(A-14)}$$

where all the terms independent of $\{u_i\}$ have been lumped with c_n in d_n. Since P_n and $\hat{R}$ are both symmetric, $\tilde{R}_n^{-1}$ is symmetric. Therefore, (A-14) can be simplified further to obtain:

$$J_n^* = \frac{1}{2} E \{x_n'[\phi' P_n \phi - G_n \tilde{R}_n^{-1} G_n]$$

$$+ 2x_n'[\phi'(P_n \Gamma_2 + P_{wn} \phi_w) - G_n' \tilde{R}_n^{-1} G_{wn}] w_n\} + d_n \qquad \text{(A-15)}$$

If we add the next term in the summation (3.11) to (A-15) we have:

$$J_{n-1}(u_{n-1}) = \frac{1}{2} E \{x_n'(\hat{Q} + \phi' P_n \phi - G_n' \tilde{R}_n^{-1} G_n) x_n$$

$$+ 2x_n'[\hat{N} + \phi'(P_n \Gamma_2 + P_{wn} \phi_w) - G_n' \tilde{R}_n^{-1} G_{wn}] w_n$$

$$+ 2x_{n-1}' \hat{M} u_{n-1} + u_{n-1} \hat{R} u_{n-1}\} + d_n \qquad \text{(A-16)}$$

But, utilizing (3.13), this can be rewritten to obtain:

$$J_{n-1}(u_{n-1}) = \frac{1}{2} E \{x_n' P_{n-1} x_n + 2x_n' P_{wn-1} w_n + 2x_{n-1}' \hat{M} u_{n-1}$$

$$+ u_{n-1}' \hat{R} u_{n-1}\} + d_n \qquad \text{(A-17)}$$

Note, since d_n does not depend on $\{u_i\}$ this equation is equivalent to the previously minimized (A-1) with n replaced by n-1. Therefore, the optimization of this equation will yield the same results as before with the index decremented by one unit.

APPENDIX B

A derivation of the Kalman one-step predictor equations is presented here. The interested reader is refered to references [9-11, 14-19] for further, more in depth information concerning the exact mathematical descriptions and properties of the Kalman estimator. The presentation here follows [11].

We begin by presenting three identities [11] used extensively in the derivation. They are:[1]

$$E\{x|y, \underline{z}\} = E\{x|y, \tilde{\underline{z}}\} \tag{I-1}$$

$$E\{x|y, \tilde{\underline{z}}\} = E\{x|y\} \cdot E\{x|\tilde{\underline{z}}\} - \bar{x} \tag{I-2}$$

$$E\{x|y\} = \bar{x} + P_{xy}P_{yy}^{-1}(y-\bar{y}) \tag{I-3}$$

where the P's are covariances defined by:

$$P_{xy} = E\{(x-\bar{x})(y-\bar{y})'\} \quad \text{and} \quad P_{yy} = E\{(y-\bar{y})(y-\bar{y})'\}$$

and $\tilde{\underline{z}}$ is the estimation error given by:

$$\tilde{\underline{z}} = \underline{z} - \hat{\underline{z}} \tag{I-4}$$

where $\underline{z}$ is the actual value and $\hat{\underline{z}}$ the predicted estimate.

Next, in order to simplify writing the expressions all the augmented system matrices are defined by single symbols. These definitions are given below with all unmentioned quantities retaining their previous definitions as given in Chapter 3.

---

[1] x,y and $\underline{z}$ are gaussian random variables; the bar denotes mean value.

$$\hat{x}_{Ak} = \begin{bmatrix} \hat{x}_k \\ \hat{w}_k \end{bmatrix} , \phi_A = \left[\begin{array}{c|c} \phi & \Gamma_2 \\ \hline 0 & \phi_w \end{array}\right] , \Gamma_A = \begin{bmatrix} \Gamma_1 \\ 0 \end{bmatrix} , C_A = [C : C_w] , \xi_{Ak} = \begin{bmatrix} \xi_k \\ \eta_k \end{bmatrix} .$$

Note, the subscript A denotes an augmented quantity.

These shorthand notations are used during the derivation to simplify writing some of the intermediate equations. In the summary, the final equations are put into a form consistant with the augmented system equations of section 3.

Beginning with the definition of the one-step predicted estimate:

$$\hat{x}_{Ak+1} = E\{x_{k+1} | y_o, \ldots, y_k\} \tag{B-1}$$

we substitute the value of x_{Ak+1} given by (3.16) to obtain:

$$\hat{x}_{Ak+1} = E\{\phi_A x_{Ak} | y_o, \ldots, y_k\} + E\{\Gamma_A u_k | y_o, \ldots, y_k\}$$
$$+ E\{\xi_{Ak} | y_o, \ldots, y_k\} \tag{B-2}$$

where the expected value of a sum property was also used.

Next, since ξ_{Ak} and $(y_o, \ldots, y_k)$ are uncorrelated, zero-mean, gaussian, random variables, the last term in (B-2) is zero. Therefore, utilizing identities (I-1) and (I-2), (B-2) can be written as follows:

$$\hat{x}_{Ak+1} = \phi_A E\{x_{Ak} | y_o, \ldots, y_{k-1}\} + \phi_A E\{x_{Ak} | \tilde{y}_k\}$$
$$+ \Gamma_A E\{u_k | y_o, \ldots, y_k\} \tag{B-3}$$

where ϕ_A and Γ_A have been removed from the expectation operation since they are deterministic. Note, the first term in (B-3) is simply the definition of the one-step predicted estimate at time k; and, given the measurements $(y_o, \ldots, y_k)$, u_k is completely determined. Therefore, (B-3) becomes:

$$\hat{x}_{Ak+1} = \phi_A \hat{x}_{Ak} + \Gamma_A u_k + \phi_A E\{x_{Ak} | \tilde{y}_k\} \tag{B-4}$$

Applying identity (I-3) to the third term in (B-4), we obtain:

$$E\{x_{Ak}|\tilde{y}_k\} = E\{x_{Ak}\tilde{y}_k'\} \quad (E\{\tilde{y}_k\tilde{y}_k'\})^{-1}\tilde{y}_k \tag{B-5}$$

since $\tilde{y}_k$ and x_{Ak} have zero means.

Substitution of (B-5) into (B-4) yields:

$$\hat{x}_{Ak+1} = \phi_A\hat{x}_{Ak} + \Gamma_A u_k + L_k(y_k - \hat{y}_k) \tag{B-6}$$

where the definition of the estimation error of y_k was used and,

$$L_k = \phi_A E\{x_{Ak}\tilde{y}_k'\} \quad (E\{\tilde{y}_k\tilde{y}_k'\})^{-1} \tag{B-7}$$

This can be further simplified by utilizing the definition of the predicted estimate and the value of y_k given by (3.17) to obtain:

$$\hat{y}_k = E\{y_k|y_o,\ldots, y_{k-1}\} = C_A\hat{x}_{Ak} + E\{v_k|y_o,\ldots, y_{k-1}\} \tag{B-8}$$

However, v_k and $(y_o,\ldots, y_k)$ are uncorrelated. Hence:

$$\hat{y}_k = C_A\hat{x}_{Ak} \tag{B-9}$$

since v_k has a zero mean. Substitution of this into (B-6) yields:

$$\hat{x}_{Ak+1} = \phi_A\hat{x}_{Ak} + \Gamma_A u_k + L_k(y_k - C_A\hat{x}_{Ak}) \tag{B-10}$$

The problem now becomes one of defining L_k in terms of the system matrices. First, consider:

$$\tilde{y}_k = y_k - C_A\hat{x}_{Ak} = C_A\tilde{x}_{Ak} + v_k \tag{B-11}$$

where this was obtained through the use of (B-9), the definition of $\tilde{y}_k$ and equation (3.17) defining y_k.

Utilizing (B-11), we can write:

$$E\{x_{Ak}\tilde{y}_k'\} = E\{x_{Ak}(C_A\tilde{x}_{Ak})'\} + E\{x_{Ak}\, v_k'\} \tag{B-12}$$

Since x_{Ak} and v_k are uncorrelated, zero mean, random variables, the last term is zero. Utilizing the definition of the estimation error, the remaining term becomes:

$$E\{x_{Ak}\tilde{y}_k'\} = E\{\hat{x}_{Ak}\tilde{x}_{Ak}'C_A'\} + E\{\tilde{x}_{Ak}\tilde{x}_{Ak}'C_A'\} \tag{B-13}$$

However, the estimation error and the estimate are uncorrelated, zero mean, random variables. Therefore, their cross-correlation is equal to zero. Hence,

$$E\{x_{Ak}\tilde{y}_k'\} = \Sigma_k C_A' \tag{B-14}$$

where $\Sigma_k = E\{\tilde{x}_{Ak}\tilde{x}_{Ak}'\}$.

Next, utilizing (B-11) we have:

$$E\{\tilde{y}_k\tilde{y}_k'\} = E\{(C_A\tilde{x}_{Ak} + v_k)(C_A\tilde{x}_{Ak} + v_k)'\} \tag{B-15}$$

Since $\tilde{x}_{Ak}$ and v_k are zero mean, uncorrelated, random variables; the expansion of (B-15) yields:

$$E\{\tilde{y}_k\tilde{y}_k'\} = C_A\Sigma_k C_A' + \Theta_k \tag{B-16}$$

where $\Theta_k = E\{v_k\, v_k'\}$.

Therefore, substitution of (B-14) and (B-16) into (B-7) defining L_k yields:

$$L_k = \phi_A\Sigma_k C_A'[C_A\Sigma_k C_A' + \Theta_k]^{-1} \tag{B-17}$$

which is the desired result.

The last part of the derivation involves obtaining an expression for Σ_k. This process begins with the definition of the error covariance and that of $\tilde{x}_{Ak}$ to obtain:

$$\Sigma_{k+1} = E\{\tilde{x}_{Ak+1}\tilde{x}_{Ak+1}\} = E\{(x_{Ak+1} - \hat{x}_{Ak+1})(x_{Ak+1} - \hat{x}_{Ak+1})'\} \tag{B-18}$$

Expansion of the above using the state equations for x_{Ak+1} and $\hat{x}_{Ak+1}$ given by (3.16) and (B-10) yields:

$$\Sigma_{k+1} = E\{(\phi_A\tilde{x}_{Ak} + \xi_{Ak} - L_k[y_k - C_A\hat{x}_{Ak}])(\phi_A\tilde{x}_{Ak} + \xi_{Ak} - L_k [y_n - C_A\hat{x}_{Ak}])\} \tag{B-19}$$

or using (B-11):

$$\Sigma_{k+1} = E\{(\phi_A \tilde{x}_{Ak} + \xi_{Ak} - L_k \tilde{y}_k)(\phi_A \tilde{x}_{Ak} + \xi_{Ak} - L_k \tilde{y}_k)\} \quad \text{(B-20)}$$

Noting that $\tilde{x}_{Ak}$ and ξ_{Ak} are uncorrelated, the expansion of (B-20) yields:

$$\Sigma_{k+1} = E\{\phi_A \tilde{x}_{Ak} \tilde{x}'_{Ak} \phi_a - \xi_{Ak}(L_k \tilde{y}_k)' - \phi_A \tilde{x}_{Ak}(L_k \tilde{y}_k)' + \xi_{Ak}\xi'_{Ak}$$

$$- L_k \tilde{y}_k (\phi_A \tilde{x}_{Ak})'$$

$$- L_k \tilde{y}_k \xi'_{Ak} + L_k \tilde{y}_k \tilde{y}'_k L'_k\} \quad \text{(B-21)}$$

Since $\tilde{x}_{Ak}$ and v_k are uncorrelated, the terms involving $(\tilde{x}_{Ak}, \tilde{y}_k)$ can be written as follows:

$$E\{\tilde{x}_{Ak} \tilde{y}'_k\} = E\{\tilde{x}_{Ak}(C \tilde{x}_{Ak} + v_k)'\} = \Sigma_k C'_A \quad \text{(B-22)}$$

If we define:

$$E\{\xi_{Ak} \xi'_{Ak}\} = \Xi_k \quad \text{(B-23)}$$

and make use of (B-16) for $E\{\tilde{y}_k \tilde{y}'_k\}$, (B-23) becomes:

$$\Sigma_{k+1} = \phi_A \Sigma_k \phi'_A - \phi_A \Sigma_k C'_A L_k - L_k C_A \Sigma_k \phi'_A + L_k (C_A \Sigma_k C'_A + \Theta_k) L'_k$$

$$+ \Xi_k + E\{- \xi_{Ak}(L_k \tilde{y}_k)' - L_k \tilde{y}_k \xi_{Ak}\} \quad \text{(B-24)}$$

Looking at the last term, we note that ξ_{Ak} and $\tilde{y}_k$ are uncorrelated. Therefore, their cross-correlation is zero due to the fact that they possess zero mean values. Hence, substitution of L_k given by (B-17) into (B-24) yields:

$$\Sigma_{k+1} = \phi_A \Sigma_k - \Sigma_k C'_A [C_A \Sigma_k C'_A + \Theta_k]^{-1} C_A \Sigma_k \phi'_A + \Xi_k \quad \text{(B-25)}$$

This equation is identical to the desired result and the derivation is complete. The one-step prediction equations derived in this section are rewritten below using the augmented system matrices. Note,

they are identical to those given in section 3.

$$\begin{bmatrix} \hat{x}_{k+1} \\ \hat{w}_{k+1} \end{bmatrix} = \begin{bmatrix} \phi & \Gamma_2 \\ 0 & \phi_w \end{bmatrix} \begin{bmatrix} \hat{x}_k \\ \hat{w}_k \end{bmatrix} + \begin{bmatrix} \Gamma_1 \\ 0 \end{bmatrix} u_k + L_k \left[y_k - [C \mid C_w] \begin{bmatrix} \hat{x}_k \\ \hat{w}_k \end{bmatrix} \right]$$

where

$$L_k = \begin{bmatrix} \phi & \Gamma_2 \\ 0 & \phi_w \end{bmatrix} \Sigma_k [C \mid C_w]' \left[[C \mid C_w] \Sigma_k [C \mid C_w]' + \Theta_k \right]^{-1} ,$$

$$\Sigma_k = E\left\{ \begin{bmatrix} \tilde{x}_k \\ \tilde{w}_k \end{bmatrix} \begin{bmatrix} \tilde{x}_k \\ \tilde{w}_k \end{bmatrix}' \right\}, \quad \begin{bmatrix} \tilde{x}_k \\ \tilde{w}_k \end{bmatrix} = \begin{bmatrix} x_k \\ w_k \end{bmatrix} - \begin{bmatrix} \hat{x}_k \\ \hat{w}_k \end{bmatrix} ,$$

and Σ_k is given by the solution of

$$\Sigma_{k+1} = \begin{bmatrix} \phi & \Gamma_2 \\ 0 & \phi_w \end{bmatrix} \left[\Sigma_k - \Sigma_k [C \mid C_w]' \left[[C \mid C_w] \Sigma_k [C \mid C_w]' + \Theta_k \right]^{-1} [C \; C_w] \Sigma_k \right] \begin{bmatrix} \phi & \Gamma_2 \\ 0 & \phi_w \end{bmatrix}' + \Xi_k ,$$

where,

$$\Xi_k = E\left\{ \begin{bmatrix} \xi_k \\ \eta_k \end{bmatrix} \begin{bmatrix} \xi_k \\ \eta_k \end{bmatrix}' \right\}$$

$$\Theta_k = E\{v_k v_k'\} .$$

REFERENCES

[1] R.H. Foulkes, Jr., "Digital Flight Compensation for Descending Constant Velocity Spiral Paths," Final report, NASA Grant NSG1199.

[2] B. Etkin, Dynamics of Atmospheric Flight. New York: John Wiley and Sons, Inc., 1972.

[3] J. Roskam, Flight Dynamics of Rigid and Elastic Airplanes. Roskam Aviation and Engineering Corp., 519 Boulder, Lawrence, Kansas, 1972.

[4] A. Papoulis, Probability, Random Variables, and Stochastic Processes. New York: McGraw-Hill Book Company, 1965.

[5] W.F. Hodge and W.H. Bryant, "Monte Carlo Analysis of Inaccuracies in Estimated Aircraft Parameters Caused by Unmodeled Flight Instrumentation Errors," NASA TN D-7712, Feb., 1975.

[6] W.C. Hoffman, W.M. Hollister, and R.W. Simpson, "Functional Error Analysis and Modeling for ATC System Concepts Evaluation," Aerospace Systems, Inc., Report No. DOT-TSC-212-72-1, May, 1972.

[7] N. Halyo and A. Caglayan, "On the Discrete-time Equivalent of the Stochastic Linear-Quadratic-Gaussian Sampled-Data Regulator Problem," submitted for publication.

[8] N. Halyo and R.H. Foulkes, "On the Quadratic Sampled-Data Regulator with Unstable Random Disturbances," 1974 International Conference of IEEE Systems, Man and Cybernetics Society, Dallas, Texas, 1974.

[9] M. Athans, "The Role and Use of the Stochastic Linear-Quadratic-Gaussian Problem in Control System Design," IEEE Trans. Auto. Control, vol. AC-16, pp 529-552, 1971.

[10] A.E. Bryson and Y. Ho, Applied Optimal Control. New York: John Wiley and Sons, 1975.

[11] J.S. Meditch, Stochastic Optimal Linear Estimation and Control. New York: McGraw-Hill Book Company, 1969.

[12] P. Dorato and A.H. Lewis, "Optimal Linear Regulators: The Discrete-time Case," IEEE Trans. Auto. Control, vol. AC-16, pp 613-620, 1971.

[13] T.L. Gunckel II and G.F. Franklin, "A General Solution for Linear Sampled-Data Control," Trans. ASME, JRN. Basic Engr. vol. 85, pp 197-201, June 1963.

[14] P.D. Joseph and J.T. Tou, "On Linear Control Theory," AIEE Trans. (Appl. Ind.), vol. 80, pp 193-196, Sept. 1961.

[15] E. Tse, "On the Optimal Control of Stochastic Linear Systems," IEEE Trans. Auto. Control, vol. AC-16, pp 776-785, 1971.

[16] H.J. Kushner, Introduction to Stochastic Control. New York: Holt, Rinehart, and Winston, 1971.

[17] R.E. Kalman, "A New Approach to Linear Filtering and Prediction Problems," Trans. ASME JRN. Basic Engr., vol. 82, pp 34-45, March, 1960.

[18] R.E. Kalman and R.S. Bucy, "New Results in Linear Filtering and Prediction Theory," Trans. ASME JRN. Basic Engr., vol. 83, pp 95-107, March, 1961.

[19] Ian B. Rhodes, "A Tutorial Introduction to Estimation and Filtering," IEEE Trans. Auto. Control, vol. AC-16, pp 688-706, 1971.